Evidence for Baseline Retinal Pigment Epithelium Pathology in the Trp1-Cre Mouse

Evidence for baseline retinal pigment epithelium pathology in the Trp1-Cre mouse

Aristomenis Thanos, Yuki Morizane, Yusuke Murakami, Andrea Giani, Dimosthenis Mantopoulos, Maki Kayama, Mi In Roh, Norman Michaud, Basil Pawlyk, Michael Sandberg, Lucy H. Young, Joan W. Miller, and Demetrios G. Vavvas[1]

From the Retina Service, Angiogenesis Laboratory, Massachusetts Eye and Ear Infirmary, Department of Ophthalmology, Harvard Medical School, Boston, Massachusetts, 02114, USA

[1]**Corresponding author:**

Demetrios G. Vavvas, M.D., Ph.D.,

Retina Service, Angiogenesis Laboratory, Massachusetts Eye and Ear Infirmary, Harvard Medical School, 243 Charles St., Boston, Massachusetts, 02114, USA

Phone: 617 573 6874 Fax 617-573-3011

E-mail: vavvas@meei.harvard.edu

Manuscript information: The number of text pages: 28, of figures: 9, and of tables: 1.

Abstract

The increasing popularity of the Cre/loxP recombination system has lead to the generation of numerous transgenic mouse lines in which Cre recombinase is expressed under the control of organ or cell-specific promoters. Alterations in retinal pigment epithelium (RPE) are prevalent in the pathogenesis of a number of ocular disorders, including age-related macular degeneration. To date, six transgenic mouse lines have been developed that target Cre to the RPE under the control of various gene promoters. However, multiple lines of evidence indicate that high levels of Cre expression can be toxic to mammalian cells. We report here that in the Trp1-Cre mouse, a commonly used transgenic Cre strain for RPE gene function studies, Cre recombinase expression alone leads to RPE dysfunction and concomitant disorganization of RPE layer morphology, large areas of RPE atrophy, retinal photoreceptor dysfunction, and microglial cell activation in the affected areas. The phenotype described herein is similar to previously published reports of conditional gene knockouts utilizing the Trp1-Cre mouse, suggesting that Cre toxicity alone could account for some of the reported phenotypes and highlights the importance to include Cre-expressing mice as controls in conditional gene targeting studies.

Introduction

The retinal pigment epithelium (RPE) is a multifunctional, cuboidal monolayer of cells that separates the retinal photoreceptors from the choroid. The RPE is an essential component of the vertebrate retina and perform diverse functions including the formation of the outer blood retinal barrier, the phagocytosis of photoreceptor outer disk segments, and the regeneration of 11-*cis* retinal for the visual cycle.(1,2) Dysfunction of the RPE has been linked with a variety of ocular disorders, including age-related macular degeneration and retinitis pigmentosa, among others.

The Cre-loxP recombination system has been instrumental in dissecting the spatial and temporal function of many important genes involved in development, physiology or disease through the generation of organ or cell-specific knock out animals. It is an elegant technique to bypass lethal or severe developmental defects resulting from systemic ablation of essential genes.(3) Cre recombinase is a 38-kDa protein that catalyzes the recombination between two of its loxP recognition sites, a 34 bp sequence consisting of a core 8 bp sequence and two 13 bp palindromic flanking sequences.(4) However, several lines of evidence indicate that Cre expression can be toxic in mammalian cells since it can cleave mammalian DNA in a nonspecific manner at sequences sharing limited homology with the 34 bp loxP sequence.(5) Pseudo/cryptic-loxP sites that occur naturally in *Escherichia coli*, yeast and mammalian genomes serve as low affinity substrates for Cre recombinase (6-8) and continuous exposure to high concentrations of the enzyme triggers cleavage and recombination between these sites. These “illegitimate” recombinations can result in growth inhibition, cell cycle arrest, DNA strand breaks or even gross chromosomal aberrations.(9-11)

Here, we report the phenotype induced by Cre expression in the RPE of the Trp1-Cre transgenic mouse strain, where Cre is expressed under the control of tyrosinase related protein 1 (Trp1/Tyrp1, hereafter referred as Trp1) gene promoter. Trp1 belongs to the tyrosinase family of proteins, which are uniquely expressed in melanin synthesizing cells, including the RPE. Trp1 is a glycoprotein located in the melanosomal membrane that acts within the context of a series of reactions in the melanogenic pathway to control melanin production in melanosomes.(12) In this manuscript we describe damage to RPE and retina in the Trp1-Cre mouse that includes drastic changes in gross cellular and ultrastructural morphology, irregularities in gene expression and ERG abnormalities; these alterations are not exhibited in their littermate controls.

Materials & Methods

Animals

All animal experiments followed the guidelines of the ARVO Statement for the Use of Animals in Ophthalmic and Vision Research and were approved by the Animal Care Committee of Massachusetts Eye and Ear Infirmary. The transgenic mouse line expressing Cre recombinase under the control of the Trp1 promoter was used for the experiments.(13) Genotyping of the Trp1-Cre transgenic allele was performed with the following primer set: Trp1-CreF, 5′-GCGGTCTGGCAGTAAAAACTATC-3′ and Trp1-CreR, 5′-GTGAAACAGCATT GCTGTCACTT-3′ along with an internal control primer set: CTAGGCCACAG AATTGAAAGATCT and′5 -GTAGGTGGAAATTCTAGCATCATCC-3′, which produced amplicons of 102 and 324 bp, respectively (See Supplementary Figure 1A at http://ajp.amjpathol.org). The Trp1-Cre mouse strain was backcrossed for at least 10 generations with C57Bl/6 mice. All mice harboring the Trp1-Cre transgene were genotyped for the rd1 (retinal degeneration 1; rd1) mutation (14) and only mice that did not carry the mutation where used for the experiments. Genomic DNA from FVB/N mice was obtained from Jackson Laboratories (Bar Harbor, Maine) and used as a positive control for the rd1 mutation. (See Supplementary Figure 1B at http://ajp.amjpathol.org) Littermate mice not carrying the Cre transgene were used as controls for all experiments. The ROSA26R reporter gene mouse was obtained from Jackson laboratories.(15) Anesthesia was achieved by intraperitoneal injection of 50 mg/kg ketamine hydrochloride (Phoenix Pharmaceutical, Inc., St. Joseph, MO) and 10 mg/kg xylazine (Phoenix Pharmaceutical, Inc.), and pupils were dilated with topical 0.5% tropicamide (Alcon, Humacao, Puerto Rico)

Immunohistochemistry of RPE flatmounts

Under deep anesthesia mice were perfused through the left ventricle with 10 ml PBS followed by 10 ml of 4% parafolmadehyde (PFA). Eyes were enucleated and the anterior segment and retina were removed under a dissecting microscope. Special attention was paid during the removal of the retina to avoid damage of the underlying RPE. Four relaxing radial incisions were made and the remaining RPE-choroid-sclera complex was flat mounted on a glass slide. Flatmounts were air-dried for 10 min and incubated for 1 hr with blocking solution (5% donkey serum, 0.3% bovine serum albumin, 0.3% Triton-X). Primary antibodies were incubated overnight at 4°C in a moisture chamber. A full list of antibodies as well as their working concentrations is in Supplemental Table 1 at http://ajp.amjpathol.org.

X-Gal Staining for β-Galactosidase Activity

For whole-mount X-Gal staining, eyes were enucleated and fixed for 7 min in 4% PFA. After fixation, eyes were washed thoroughly three times with wash buffer (0.1 M sodium phosphate, 2 mM $MgCl_2$, 0.01% deoxycholate, 0.02% Nonidet P-40). Immediately after washing, eyes were placed in pre-warmed (37°C) X-Gal staining solution (5 mM $K_3Fe(CN)_6$, 5 mM $K_4Fe(CN)_6$-$6H_2O$ diluted in wash buffer) and X-Gal (5-bromo-4-chloro-3-indolyl β-D-galactopyranoside, SIGMA) was added to a final concentration of 1 mg/ml. Eyes were protected from light and incubated in 37°C overnight. For tissue sections, eyes were enucleated and embedded into optimal temperature cutting medium (OCT-TissueTek). Serial sections of 10 µm were cut using

a cryostat (Leica) and assayed for β-galacatosidase activity, as described above. To better visualize X-gal staining in the RPE, pigment was bleached (after X-gal staining) by incubation in KMnO4 (0.25% in water) for 35 min at room temperature (protected from light) and subsequent incubation in oxalic acid (1% in water) for 20 min at room temperature.

Fluorescein Angiography (FA)

FA was performed using a commercial camera and imaging system (TRC 50 VT camera and IMAGEnet 1.53 system; Topcon, Paramus, NJ). Photographs were captured with a 20-diopter lens in contact with the fundus camera lens after intraperitoneal injection of 0.1 mL of 2% fluorescein sodium (Akorn, Decatur, IL).

ERG Analysis

ERGs were recorded as previously described (16). Briefly, following an overnight dark adaptation mice were anesthetized with sodium pentobarbital at 80 mg/kg given intraperitoneally. Their pupils were dilated with 0.2% phenylephrine and 0.02% cyclopentolate hydrochloride. Full-field, rod-dominant (>95%) ERGs were elicited with 10 μsec flashes of white light (4.3 log ft-Lt) presented at 1-minute intervals in a Ganzfeld dome.

Electron Microscopy

Eyes were enucleated under deep anesthesia and the globe was cleaned of all extraneous tissue then rinsed with saline. The globe was immediately placed into fixative consisting

of 2.5% gluteraldehyde and 2% formaldehyde in 0.1 M cacodylate buffer with 0.08 M $CaCl_2$ at 4 °C. After a short 10 to 15 min fixation, the eye was bisected at the limbus and the anterior segment was separated from the posterior segment and the parts to be examined were placed back in the fixative. Within 24 hr of enucleation, the tissue was washed in 0.1 M cacodylate buffer and stored at 4°C. The tissue was post-fixed for 1.5 hr in 2% aqueous OsO_4. Tissue was dehydrated in graded ethanols, transitioned in propylene oxide, infiltrated with propylene oxide and epon mixtures (TAAB 812 resin, Marivac, Quebec, Canada) embedded in epon and cured for 48 hr at 60°C. One-micron sections were cut on a Leica Ultracut UCT and stained with 1% toluidine blue in 1% borate buffer. For transmission electron microscopy observation, thin sections were cut at 70-90 nm and stained with saturated, aqueous uranyl acetate and Sato's lead stain. Examination was done on a Philips CM-10 electron microscope.

Animal SD-OCT

Optical coherence tomography was performed using a spectral domain OCT system (SDOCT Bioptigen Inc., Durham, NC) as previously described.(17) Briefly, a volume analysis centered on the optic nerve head was performed, using 100 horizontal, raster, and consecutive B-scan lines, each one composed by 1200 A-scans. The volume size was 1.6 x 1.6 mm. Total retinal thickness and outer nuclear layer thickness was assessed at 500 µm, 400 µm, 300 µm distance from the optic nerve head (nasally and temporally) and at 200 µm, 400 µm above and below the optic nerve head.

Western Blot analysis

The choroid-RPE tissue from Trp1-Cre mice and respective controls was separated from the retina and homogenized in lysis buffer(18), supplemented with a mixture of proteinase inhibitors (Complete Mini; Roche Diagnostics, Basel, Switzerland). The samples were centrifuged (14,000 rpm for 30 min at 4°C) and supernatants were collected. Protein concentration was assessed with the bicinchoninic acid protein assay (BCA, Pierce, Rockford, IL, USA). Thirty micrograms of protein per sample were separated in a 4-20% gradient sodium dodecyl sulfate-polyacrylamide gel (SDS-PAGE) (Invitrogen Corporation, Carlsbad, CA, USA) electrophoresis and the proteins were electroblotted onto PVDF membranes. After 20 min incubation in blocking solution (Starting Block ^{TM}T20, Thermo Scientific, Waltham, MA), membranes were incubated with primary antibodies overnight at 4°C. Supplemental table 1 includes a full list of antibodies and their working concentrations. Peroxidase-labeled secondary antibodies (Amersham Pharmacia Biotech, Piscataway, NJ, USA) were used and proteins were visualized with enhanced chemiluminescence technique (Amersham Pharmacia Biotech).

ELISA

Analysis of IL-10 production was performed using a quantitative ELISA kit (R&D Systems). After perfusion with 10 ml PBS, choroid-RPE lysates from wild type and Trp1-Cre mice were collected and assayed for IL-10 protein levels according to the manufacturer's instructions. Values were normalized to lysate protein levels.

Statistical Analysis

Values are expressed as mean ± SEM (unless specified), and statistical analysis was performed using an un-paired Student t-test (***, $P < 0.001$; **, $P < 0.01$; *, $P < 0.05$; ns, $P > 0.05$).

Results

Expression pattern of Cre-recombinase in the Trp1-*Cre* mouse

To evaluate the expression pattern of Cre recombinase in the Trp1-Cre transgenic mouse strain, adult 2 month old Trp1-Cre mice were crossed with the ROSA26 reporter gene mouse to yield a Trp1-Cre;ROSA26R line. Upon Cre gene expression, the recombinase activity results in the excision of a loxP-flanked STOP sequence that prevents expression of a lacZ gene.(15) Thus, β-galactosidase staining reflects Cre recombinase activity *in vivo*. We confirmed that the Trp1-Cre mouse provided robust Cre expression in the RPE (Fig.1C). To estimate the percentage of Cre- expressing cells, X-Gal staining and subsequent melanin bleaching were performed on whole eyecups of Trp1-Cre;ROSA26R mice. There was a variable degree of mosaicism in Cre-expression ranging from 60 to 90% of total RPE cells (Fig.1F, Supplementary Fig. 1C at http://ajp.amjpathol.org). Ectopic Cre expression in other ocular tissues was evident such as the ciliary margin of the retina (Fig. 1A, B, E), ciliary pigment epithelium (Fig. 1B) and optic nerve stalk (See Supplementary Fig. 1D at http://ajp.amjpathol.org). ROSA26R eyecups incubated with X-Gal staining solution did not show any β-galactosidase activity. (Fig. 1G, H) Taken together, these data indicate that the expression pattern of our Trp1-Cre strain is consistent with the one described by Mori et al in the initial description of the Trp1-Cre mouse.(13)

Severely altered RPE morphology in the Trp1-Cre mouse

Intercellular tight junctions are critical for the maintenance of RPE monolayer integrity. Adherens proteins, such as β-catenin, are important for intercellular adhesion and preservation of the epithelial morphology, whereas tight junction proteins, like zona occludens-1 (ZO-1), have a fundamental role for the formation and function of outer blood retinal barrier.(19) To examine the morphology of the RPE layer in the Trp1-Cre mouse, immunofluorescent staining was performed on flatmounts using a monoclonal antibody against the adherens junction protein β-catenin. In Trp1-Cre mice, the majority of the RPE monolayer had lost its classic honey-comb appearance and the cells were enlarged, polygonal, and dysmorphic compared to wild type controls (Fig. 2A-F). Quantitative analysis showed a dramatic decrease in RPE cell density (number of cells per unit area)(Fig. 2G). Average cell size and perimeter were found to be significantly higher in Trp1-Cre mice compared to wild types (Fig.2H, I). Similar results were obtained after immunostaining with a FITC-conjugated monoclonal antibody against ZO-1 (See Supplemental Fig. 2A at http://ajp.amjpathol.org). Furthermore, although β-catenin is mostly associated with the cell membrane, an aberrant cytoplasmic distribution was evident indicating a disturbance in its characteristic membranous association (Fig. 2D, F arrows). The latter was accompanied by a reduction of protein expression as shown by Western blot on 2-month-old choroid-RPE lysates. (Fig. 2K, L). Finally, immunofluorescent staining with a mouse monoclonal antibody against Cre recombinase revealed nuclear localization of the protein as expected. (Fig. 2F).

Pigmentary defects in the RPE of the Trp1–Cre mouse

Macroscopic examination of RPE flatmounts from Trp1-Cre mice revealed wedge-shaped areas of pigmentary defects that were extending from the mid-periphery until the ora serrata (Fig.3B, arrows). To further examine this finding, FA was performed in adult 1-month-old animals. The pigmentary defects observed previously corresponded to areas of hyperfluoresence that increased in intensity over time but not in size (window defect) (Fig.3F, G, H, arrows). These defects were bilateral and interestingly found at all times in similar position in the periphery of the eye (2 and 10 o'clock meridians). In addition, late phase angiograms of Trp1-Cre mice revealed diffuse background hyperfluorescence (Fig.3G, H). Next, Trp1-Cre and wild type littermate controls were perfused with rhodamine-conjugated concanavalin-A lectin and counterstained the overlying RPE layer with a FITC-conjugated antibody against ZO-1 (Fig.3I-N). As expected, in wild-type animals the RPE layer precluded visualization of the underlying choroid due to its dense melanin content (Fig.3I-K), whereas in Trp1-Cre mice the choroidal vasculature was visible beneath the RPE indicating a defect in its pigmentation (Fig.3L-N), which may account, at least in part, for the diffuse background hyperfluorescence observed on FA. This was further supported from 1μm semi-thin sections stained with toluidine blue, where the RPE layer was flattened with large discontinuities in its pigmentation (Fig. O-Q).

Morphological abnormalities in the RPE of the Trp1-Cre mice

Next, the morphology of the RPE layer was assessed by transmission electron microscopic analysis of adult 2-month-old wild type and Trp1-Cre mice. There was a

substantial decrease in the thickness of RPE cells of Trp1-Cre mice with either loss or disorganization of the apical villi, which did not integrate with the outer segments of photoreceptors (Fig.4D-I, asterisk). In addition, a reduction of basal laminar infoldings was noted (Fig. 4E-H). Melanin granules were larger (Fig. 4E,F) and irregularly shaped (Fig.4E,H) compared to the elliptical or spherical shape of wild type controls (Fig 4A-C). RPE cells with little or no melanin granules were also evident (Fig.4D, G, I). In line with the initial description of the Trp1-Cre mouse, there were no abnormalities in the shape of choroidal melanocytes (Fig.4B, E-G), which do not express Cre recombinase (13).

Retinal abnormalities in Trp1-Cre mice

Given the critical role of the RPE in the maintenance and function of the photoreceptor cell layer, retinal function of Trp1-Cre mice was examined. ERG analysis was performed on adult 1-month-old animals. Both scotopic and photopic responses were significantly reduced in Trp1-Cre mice compared to the ERG responses obtained from wild type mice counterparts (Fig. 5A). To assess whether there is a progressive degeneration of photoreceptors aged 4-month-old mice were analyzed and their ERG responses compared with that of 1-month-old animals. No significant differences were identified between the ERGs of the two groups (data not shown). Consistent with the abnormal ERG data, a pronounced decrease in total retinal thickness (Fig. 5B,C) and outer nuclear layer thickness (Fig. 5B,D) was seen in Trp1-Cre mice as examined *in vivo* with Spectral Domain Optical Coherence Tomography (SD-OCT). Finally, western blot analysis of choroid-RPE lysates for RPE65, a protein abundantly expressed in the RPE

that plays a critical role in retinoid processing, revealed a significant reduction in its expression level compared to wild-type animals, suggesting possible deficits in the visual cycle (Fig. 5E).

Microglial cell activation in the Trp1-Cre mouse

The retinal microglia constitute the resident macrophages of the retina and are among the first cells to respond after tissue injury (20). Under normal conditions, the retinal microglia are distributed throughout the retinal layers with the notable exception of the subretinal space, which is considered an immune privileged site (21). To investigate whether Cre-mediated RPE damage triggers microglial cell activation, immunofluorescent staining was performed on RPE flatmounts using an antibody against the macrophage/microglial cell marker Iba-1, a calcium-binding protein involved in membrane ruffling and phagocytosis and is significantly upregulated during microglial cell activation (22). No microglial cells were detected in the subretinal space of wild type 2 month-old mice (Supplemental Fig. 3A-C at http://ajp.amjpathol.org). On the other hand, immunofluorescent staining of RPE flatmounts from Trp1-Cre mice revealed a dramatic accumulation of microglial cell in the subretinal space, mostly at the areas of the damaged RPE (Fig. 6A-F, Supplemental Figure 3 D-F at http://ajp.amjpathol.org). Furthermore, microglial cells acquired an amoeboid-like morphology with short processes (Fig. 6H) indicative of their phagocytic-activated state. Moreover, their cell bodies co-localized with cellular debris stained positive for FITC-ZO1 that was most likely originating from phagocytosed RPE cells (Fig. 6G-I, Supplemental Fig. 3 D-F at http://ajp.amjpathol.org). Finally microglial cells were

intimately associated with areas of dysfunctional RPE cell membranes or areas of RPE remodeling, as identified from the absence of ZO-1 immunostaining of RPE cell membranes or the structural changes of surrounding RPE cells, respectively (Fig 6 J-L, and Supplemental Figure 3K-M at http://ajp.amjpathol.org).

Discussion

The present study describes a phenotype in the Trp1-Cre mice characterized by dramatic changes in the morphology of the RPE monolayer, irregularities in its pigmentation, retinal dystrophy and concomitant activation of the retinal microglia in the affected areas. The described phenotype had 100% penetrance with patchy distribution and was observed in both male and female hemizygous mice for the Trp1-Cre transgene. In the Trp1-Cre strain, Cre expression in the RPE starts from embryonic day 10.5 (time of RPE differentiation) to postnatal day 12 (13) and significant changes in RPE monolayer appearance were evident also on postnatal day 14 indicating that Cre may have exerted its toxic effect even before this time point (See Supplemental Fig. 2B at http://ajp.amjpathol.org).

It is known that the insertion of a Cre transgene or any other transgene may affect the function of the upstream gene promoter chosen to drive transgene expression. For instance, CD19-Cre mice, which are employed to evaluate gene function in B-cells, show 50% decrease in the levels of CD19 expression compared to wild type B-cells (23). Similarly, rat insulin II promoter-Cre mice, expressing Cre in pancreatic β-cells, are glucose intolerant (24). Therefore, the abnormalities in RPE pigmentation and melanosome shape we observed in the Trp1-Cre mouse and previously reported by two other studies (25, 26) *may* be attributed to abnormalities in the function of Trp1 gene promoter, which drives Cre expression in this particular strain and is heavily involved in melanin synthesis under normal conditions (27).

Findings described in this study suggest that some of the phenotypes described in prior RPE specific knockout studies utilizing Trp1-Cre mice may have been a

combination of the targeted loxP gene excision and/or the Cre transgene presence toxicity itself (Table 1)(25, 26, 28-32). For instance, retinal dystrophy with abnormal ERG responses and decreased RPE65 expression have been reported by two independent studies (26, 29) using the Trp1-Cre line to knockout RXRα and Lrat, respectively, as we see in Trp1-Cre alone. Similarly, areas of hyperfluoresence that increased in intensity over time but not in size (window defect) on FA have been reported as a result of conditional ablation of VEGF in the RPE (25). In addition, the mosaic nature of the Cre toxicity phenotype necessitates that as proper controls panoramic investigation of the RPE monolayer should be included in RPE conditional knockout studies. Therefore, based on our findings in this study, we may need to re-evaluate the conclusions drawn from previous studies using the Trp1-Cre mouse (21 - 27).

Another interesting finding of this study is the activation of the retinal microglia and its subsequent migration to the subretinal space, which is normally devoid of immune cells (21). The RPE plays an important role in keeping the retinal microglia in a ramified-quiescent state through the secretion of immunosuppressive cytokines such as TGF-β, IL-10 and PEDF among others (33). Indeed, IL-10 protein levels were found to be significantly decreased in choroid-RPE lysates from Trp1-Cre mice compared to wild type controls (See Supplemental Fig. 3N at http://ajp.amjpathol.org), which may partially explain the profound activation. However, it is not clear whether the reduction in IL-10 was due to a decrease in RPE cell number or due to a general manifestation of RPE dysfunction. In our study, the retinal microglia were strongly associated with areas of damaged RPE cells and phagocytosed cellular debris most likely originating from RPE cells. It is plausible that microglial cells play a role in repopulating and remodeling the

RPE monolayer following dysfunction or cell death with the aim of maintaining its integrity. This is further supported by several recent studies demonstrating that activated subretinal microglia can influence the function of RPE cells or even change their morphology (34, 35). The accumulation of activated subretinal microglia has been demonstrated in specimens from patients with dry AMD (36). Further investigations are needed to fully elucidate the interplay between the RPE and the retinal microglia.

To date, six mouse lines expressing Cre recombinase in the RPE have been reported in the literature (13, 37-41), yet this is the first report indicating potential problems caused by prolonged and robust Cre expression by the RPE. The possibility of such toxicity effect should alert investigators utilizing other lines expressing Cre in the RPE. While the use of transgenic animals with high levels of Cre expression can ensure a high recombination level they may also pose a significant risk of Cre-mediated cellular toxicity potentially due to non-specific "illegitimate" recombination events (9). To avoid this complication, several strategies have been developed to control Cre expression such as induction via tamoxifen or tetracycline administration or the use of self-deleting Cre-expressing vectors (42). Despite these efforts, issues of toxicity remain even with ligand-dependent recombinases (43, 44). Therefore, it is clear that inclusion of the most crucial control, namely mice carrying the Cre transgene, and a comprehensive investigation of the RPE flat mount should always be included in conditional gene targeting studies for accurate interpretation of scientific results.

Acknowledgements

We thank Kip M. Connor and Patricia D'Amore for their useful advice, insightful discussions and help during the preparation of this manuscript. This work was supported by Bacardi Fund (DV), Research to Prevent Blindness Foundation (DV), Lions Eye Research Fund (DV), Onassis Foundation (DV), a Bausch & Lomb Vitreoretinal Fellowship (Y. Morizane, MK), and National Eye Institute grant EY014104 (MEEI Core Grant).

References :

1. Zinn K, Marmor MF: The retinal pigment epithelium. Cambridge, Harvard University Press, 1979.
2. Strauss, O: The retinal pigment epithelium in visual function. Physiol Rev 2005, 85:845-881
3. Nagy, A: Cre recombinase: the universal reagent for genome tailoring. Genesis 2000, 26:99-109
4. Hamilton, DL, Abremski, K: Site-specific recombination by the bacteriophage P1 lox-Cre system. Cre-mediated synapsis of two lox sites. J Mol Biol 1984, 178:481-486
5. Thyagarajan, B, Guimaraes, MJ, Groth, AC, Calos, MP: Mammalian genomes contain active recombinase recognition sites. Gene 2000, 244:47-54
6. Sauer, B: Identification of cryptic lox sites in the yeast genome by selection for Cre-mediated chromosome translocations that confer multiple drug resistance. J Mol Biol 1992, 223:911-928
7. Sauer, B: Multiplex Cre/lox recombination permits selective site-specific DNA targeting to both a natural and an engineered site in the yeast genome. Nucleic Acids Res 1996, 24:4608-4613
8. Sternberg, N, Hamilton, D, Hoess, R: Bacteriophage P1 site-specific recombination. II. Recombination between loxP and the bacterial chromosome. J Mol Biol 1981, 150:487-507
9. Loonstra, A, Vooijs, M, Beverloo, HB, Allak, BA, van Drunen, E, Kanaar, R, Berns, A, Jonkers, J: Growth inhibition and DNA damage induced by Cre recombinase in mammalian cells. Proc Natl Acad Sci U S A 2001, 98:9209-9214
10. Schmidt, EE, Taylor, DS, Prigge, JR, Barnett, S, Capecchi, MR: Illegitimate Cre-dependent chromosome rearrangements in transgenic mouse spermatids. Proc Natl Acad Sci U S A 2000, 97:13702-13707
11. de Alboran, IM, O'Hagan, RC, Gartner, F, Malynn, B, Davidson, L, Rickert, R, Rajewsky, K, DePinho, RA, Alt, FW: Analysis of C-MYC function in normal cells via conditional gene-targeted mutation. Immunity 2001, 14:45-55
12. Kobayashi, T, Hearing, VJ: Direct interaction of tyrosinase with Tyrp1 to form heterodimeric complexes in vivo. J Cell Sci 2007, 120:4261-4268
13. Mori, M, Metzger, D, Garnier, JM, Chambon, P, Mark, M: Site-specific somatic mutagenesis in the retinal pigment epithelium. Invest Ophthalmol Vis Sci 2002, 43:1384-1388
14. Gimenez, E, Montoliu, L: A simple polymerase chain reaction assay for genotyping the retinal degeneration mutation (Pdeb(rd1)) in FVB/N-derived transgenic mice. Lab Anim 2001, 35:153-156
15. Soriano, P: Generalized lacZ expression with the ROSA26 Cre reporter strain. Nat Genet 1999, 21:70-71
16. Pawlyk, BS, Bulgakov, OV, Liu, X, Xu, X, Adamian, M, Sun, X, Khani, SC, Berson, EL, Sandberg, MA, Li, T: Replacement gene therapy with a human RPGRIP1 sequence slows photoreceptor degeneration in a murine model of Leber congenital amaurosis. Hum Gene Ther 2010, 21:993-1004

17. Giani, A, Thanos, A, Roh, MI, Connolly, E, Trichonas, G, Kim, I, Gragoudas, E, Vavvas, D, Miller, JW: In-vivo evaluation of laser-induced choroidal neovascularization using spectral-domain optical coherence tomography. Invest Ophthalmol Vis Sci 2011,
18. Vavvas, D, Apazidis, A, Saha, AK, Gamble, J, Patel, A, Kemp, BE, Witters, LA, Ruderman, NB: Contraction-induced changes in acetyl-CoA carboxylase and 5'-AMP-activated kinase in skeletal muscle. J Biol Chem 1997, 272:13255-13261
19. Rizzolo, LJ: Polarity and the development of the outer blood-retinal barrier. Histol Histopathol 1997, 12:1057-1067
20. Langmann, T: Microglia activation in retinal degeneration. J Leukoc Biol 2007, 81:1345-1351
21. Jiang, LQ, Jorquera, M, Streilein, JW: Subretinal space and vitreous cavity as immunologically privileged sites for retinal allografts. Invest Ophthalmol Vis Sci 1993, 34:3347-3354
22. Kanazawa, H, Ohsawa, K, Sasaki, Y, Kohsaka, S, Imai, Y: Macrophage/microglia-specific protein Iba1 enhances membrane ruffling and Rac activation via phospholipase C-gamma -dependent pathway. J Biol Chem 2002, 277:20026-20032
23. Schmidt-Supprian, M, Rajewsky, K: Vagaries of conditional gene targeting. Nat Immunol 2007, 8:665-668
24. Lee, JY, Ristow, M, Lin, X, White, MF, Magnuson, MA, Hennighausen, L: RIP-Cre revisited, evidence for impairments of pancreatic beta-cell function. J Biol Chem 2006, 281:2649-2653
25. Marneros, AG, Fan, J, Yokoyama, Y, Gerber, HP, Ferrara, N, Crouch, RK, Olsen, BR: Vascular endothelial growth factor expression in the retinal pigment epithelium is essential for choriocapillaris development and visual function. Am J Pathol 2005, 167:1451-1459
26. Mori, M, Metzger, D, Picaud, S, Hindelang, C, Simonutti, M, Sahel, J, Chambon, P, Mark, M: Retinal dystrophy resulting from ablation of RXR alpha in the mouse retinal pigment epithelium. Am J Pathol 2004, 164:701-710
27. Kobayashi, T, Urabe, K, Winder, A, Jimenez-Cervantes, C, Imokawa, G, Brewington, T, Solano, F, Garcia-Borron, JC, Hearing, VJ: Tyrosinase related protein 1 (TRP1) functions as a DHICA oxidase in melanin biosynthesis. EMBO J 1994, 13:5818-5825
28. Westenskow, P, Piccolo, S, Fuhrmann, S: Beta-catenin controls differentiation of the retinal pigment epithelium in the mouse optic cup by regulating Mitf and Otx2 expression. Development 2009, 136:2505-2510
29. Ruiz, A, Ghyselinck, NB, Mata, N, Nusinowitz, S, Lloyd, M, Dennefeld, C, Chambon, P, Bok, D: Somatic ablation of the Lrat gene in the mouse retinal pigment epithelium drastically reduces its retinoid storage. Invest Ophthalmol Vis Sci 2007, 48:5377-5387
30. Kim, JW, Kang, KH, Burrola, P, Mak, TW, Lemke, G: Retinal degeneration triggered by inactivation of PTEN in the retinal pigment epithelium. Genes Dev 2008, 22:3147-3157
31. Fujimura, N, Taketo, MM, Mori, M, Korinek, V, Kozmik, Z: Spatial and temporal regulation of Wnt/beta-catenin signaling is essential for development of the retinal pigment epithelium. Dev Biol 2009, 334:31-45

32. Schouwey, K, Aydin, IT, Radtke, F, Beermann, F: RBP-Jkappa-dependent Notch signaling enhances retinal pigment epithelial cell proliferation in transgenic mice. Oncogene 2011, 30:313-322
33. Zamiri, P, Sugita, S, Streilein, JW: Immunosuppressive properties of the pigmented epithelial cells and the subretinal space. Chem Immunol Allergy 2007, 92:86-93
34. Ma, W, Zhao, L, Fontainhas, AM, Fariss, RN, Wong, WT: Microglia in the mouse retina alter the structure and function of retinal pigmented epithelial cells: a potential cellular interaction relevant to AMD. PLoS One 2009, 4:e7945
35. Xu, H, Chen, M, Manivannan, A, Lois, N, Forrester, JV: Age-dependent accumulation of lipofuscin in perivascular and subretinal microglia in experimental mice. Aging Cell 2008, 7:58-68
36. Gupta, N, Brown, KE, Milam, AH: Activated microglia in human retinitis pigmentosa, late-onset retinal degeneration, and age-related macular degeneration. Exp Eye Res 2003, 76:463-471
37. Le, YZ, Zheng, W, Rao, PC, Zheng, L, Anderson, RE, Esumi, N, Zack, DJ, Zhu, M: Inducible expression of cre recombinase in the retinal pigmented epithelium. Invest Ophthalmol Vis Sci 2008, 49:1248-1253
38. Aydin, IT, Beermann, F: A MART-1::Cre transgenic line induces recombination in melanocytes and RPE. Genesis 2011,
39. Iacovelli, J, Zhao, C, Wolkow, N, Veldman, P, Gollomp, K, Ojha, P, Lukinova, N, King, A, Feiner, L, Esumi, N, Zack, DJ, Pierce, EA, Vollrath, D, Dunaief, JL: Generation of Cre transgenic mice with postnatal RPE-specific ocular expression. Invest Ophthalmol Vis Sci 2011, 52:1378-1383
40. Longbottom, R, Fruttiger, M, Douglas, RH, Martinez-Barbera, JP, Greenwood, J, Moss, SE: Genetic ablation of retinal pigment epithelial cells reveals the adaptive response of the epithelium and impact on photoreceptors. Proc Natl Acad Sci U S A 2009, 106:18728-18733
41. Guyonneau, L, Rossier, A, Richard, C, Hummler, E, Beermann, F: Expression of Cre recombinase in pigment cells. Pigment Cell Res 2002, 15:305-309
42. Pfeifer, A, Brandon, EP, Kootstra, N, Gage, FH, Verma, IM: Delivery of the Cre recombinase by a self-deleting lentiviral vector: efficient gene targeting in vivo. Proc Natl Acad Sci U S A 2001, 98:11450-11455
43. Hameyer, D, Loonstra, A, Eshkind, L, Schmitt, S, Antunes, C, Groen, A, Bindels, E, Jonkers, J, Krimpenfort, P, Meuwissen, R, Rijswijk, L, Bex, A, Berns, A, Bockamp, E: Toxicity of ligand-dependent Cre recombinases and generation of a conditional Cre deleter mouse allowing mosaic recombination in peripheral tissues. Physiol Genomics 2007, 31:32-41
44. Forni, PE, Scuoppo, C, Imayoshi, I, Taulli, R, Dastru, W, Sala, V, Betz, UA, Muzzi, P, Martinuzzi, D, Vercelli, AE, Kageyama, R, Ponzetto, C: High levels of Cre expression in neuronal progenitors cause defects in brain development leading to microencephaly and hydrocephaly. J Neurosci 2006, 26:9593-9602

FIGURE LEGENDS

Figure 1. β-galactosidase activity in the Trp1-Cre;ROSA26R line. Sagittal frozen sections showing Cre expression in the ciliary margin of the retina (A-B), ciliary body (B) and retinal pigment epithelium (C). Representative RPE flatmounts from Trp1-Cre;ROSA26R mice (E-F) showing the extent of Cre expression in the peripheral retina, which was folded over for better visualization of X-Gal staining (arrows). Melanin bleaching (F-H) to identify the percentage of Cre expressing cells. No β-galactosidase activity was observed in ROSA26R controls incubated with X-Gal staining solution (D, G-H) Scale bars, A : 100 µm, B : 150 µm , C-D : 50 µm, E-H: 500 µm.

Figure 2. Morphological abnormalities of RPE monolayer of the Trp1-Cre mouse. Immunohistochemical staining for the junctional protein β-catenin revealed severe disorganization of RPE cells (C, D) with loss of its classic honeycomb appearance (A, B) Substantial loss of β-catenin membranous association (D,F arrows) was also observed compared to wild type controls. Significant decrease in cell density (G), increase in cell size and cell perimeter in Trp1-Cre mice (H-I). (K) Western blot analysis of choroid-RPE protein lysates from wild type and Trp1-Cre mice showed significant decrease in β-catenin protein expression levels. (L) Densitometric analysis of β-catenin expression. Scale Bars A,C : 50 µm, B,D-F : 200 µm

Figure 3. Pigmentary defects in Trp1-Cre mice. (A,B) Macroscopic examination of RPE flatmounts from wild type and Trp1-Cre mice showed large wedge shaped areas of

depigmentation (arrows). (C-H) Early and late phase FA demonstrated large areas of hyperfluorescence at 10' (G) and 2 o'clock (H) meridians. (I-N) Perfusion with rhodamine conjugated Concancavalin A lectin and counterstaining with FITC-ZO-1. In wild type mice, the melanin content of the RPE blocked the fluorescent signal from the choroid. In Trp1-Cre mice visualization of the underlying large bore capillary bed of the choroid can be seen due to abnormalities in its pigmentation. (O-Q) Large areas of depigmented and flattened RPE cells (arrows) were seen on 1um toluidine blue sections, compared to the uniform shape of wild type RPE cells (Q). Scale Bars, A, B : 500 µm, I-N: 50 µm, P-Q: 100 µm.

Figure 4. Ultrastructural abnormalities in the RPE of the Trp1-Cre mouse (D-I) and littermate control mice (A-C). Abnormalities in the number (D, I), shape (E) and size (F, H) of RPE melanin granules were seen in Trp1-Cre mice compared to the fusiform shape of wild type controls (A-C). Notice the unusually large melanin granule (asterisk) (F). The apical villi (AV) were collapsed and did not integrate with photoreceptors, as in wild type RPE. Microglial cell (M) with phagocytic granules in the subretinal space (E, outline). POS, photoreceptor outer segments; CC, choriocapillaris; AV, apical villi, BLI, basal laminar infoldings; BRM, Bruch's membrane; CH, choroid; M, macrophage/microglial cell Scale bars; A,B,D,I: 1 µm, C: 2 µm, E,F,G: 2.5 µm

Figure 5. Retinal abnormalities in Trp1-Cre mice. (A) Representative scotopic and photopic responses in 1-month-old control and Trp1-Cre mice. Amplitudes of both a-waves and b-waves were reduced in Trp1-Cre mice. (B) In vivo evaluation with SD-OCT

(spectral domain optical coherence tomography) at the level of optic nerve (arrow) and 200 µm above (arrowhead) and measurement of total retinal thickness (blue arrow) and outer nuclear layer thickness (orange arrow). (C-D) Significant decrease in total retinal thickness and outer nuclear layer thickness was seen in Trp1-Cre mice. (**E)** Western blot analysis of choroid-RPE lysates for RPE65 protein expression levels (n = 6).

Figure 6. Microglial cell activation and migration to the subretinal space in the Trp1-Cre mouse. (A-F) Iba-1 positive microglial cells were mostly confined to the areas of injured RPE cells. (G-I) Cellular debris stained positive for FITC-ZO1 co-localized with cell bodies of activated, amoeboid shaped microglial cells (arrows). (J-K) Microglial cells were commonly associated with areas of dysfunctional RPE cell membranes, as indicated from the absence of ZO-1 immunostaining. Scale bars, A-C: 200 µm, D-F: 100 µm, G-L: 25 µm

Supplemental Figure 1. (A) Genotyping for Cre- transgene (100 bp) and internal positive control (~324 bp) (**B)** PCR analysis for the presence of the rd1 mutation. Genomic DNA from FVB/N mice was used as positive control. (**C)** X-Gal staining and subsequent melanin bleaching of Trp1-Cre ; ROSA26R flatmounts reveals variable degree of mosaicism in Cre expression. Scale Bar : 500 µm **(D)** Wholemount X-Gal staining confirms ectopic Cre expression in the optic nerve stalk, as initially reported by Mori et al (13).

Supplemental Figure 2. (A) Double immunofluorescent staining of RPE flatmounts

from Trp1-Cre mice and littermate wild type controls using antibodies against the proteins ZO-1 and β-catenin. Loss of the classic honeycomb appearance of the RPE monolayer can be observed. Scale bar 200 µm (B) Immunofluorescent staining using an antibody against β-catenin on RPE flatmounts obtained at P14 indicates significant disorganization of the RPE monolayer. Scale bar 100 µm

Supplemental Figure 3.

Double immunofluorescent staining of RPE flatmounts using a FITC conjugated antibody against ZO-1 and the microglial cell marker Iba-1. The subretinal space is devoid of microglial cells in wild type mice (A-C), compared to Trp1-Cre mice where significant microglial cell activation is observed. (D-F) Microglial cell bodies co-localized strongly with cellular debris stained positive for FITC-ZO1. Scale Bars A-F :100 µm. Microglial were often localized in areas of RPE remodeling. Notice the changes in the shape of RPE cells (arrows) Scale Bar: 10 µm. Isotype control antibodies (K-M) Quantitative determination of IL-10 protein levels in choroid-RPE protein lysates obtained from Trp1-Cre and littermate controls (N).

Table 1. Studies that have used the Trp1-Cre mouse to inactivate targeted loxP sites

#	Targeted Gene	Phenotype described	Year	Ref.
1	RXRα	*Decreased expression of RPE65*, CRALBP • photoreceptor alterations ; decrease in number ; shortening of OS ; *reduced light responses on ERG*	2004	26
2	VEGFα	Microphthalmia • absence of choroid • *reduction in the content of melanin granules* • *abnormally shaped melanin granules* • *disorganization of basal infoldings* • *loss of apical villi* • *reduced RPE thickness* • *ERG abnormalities (decrease in a and b wave)* • *RPE defects on fluorescein angiography*	2005	25
3	Lrat	*reduced light responses on ERG* • shortening of rod outer segments • *slight reduction in photoreceptor nuclei*	2007	29
4	PTEN	Retinal degeneration • reduction in ONL • pigmented tumors in spleen	2008	30
5	β-catenin	Microphthalmia • colobomas • disruption of cellular junctions•	2009	28
6	β-catenin	Microphthalmia • colobomas • disruption of cellular junctions•	2009	31
7	RBP-Jκ, Notch1, Notch2	Microphthalmia • benign pigmented tumors	2010	32

Figure1

Trp1-Cre ROSA26R
A
B
C
D
ROSA26R
Trp1-Cre ROSA26R
ROSA26R
E
F
G
H

Figure 2

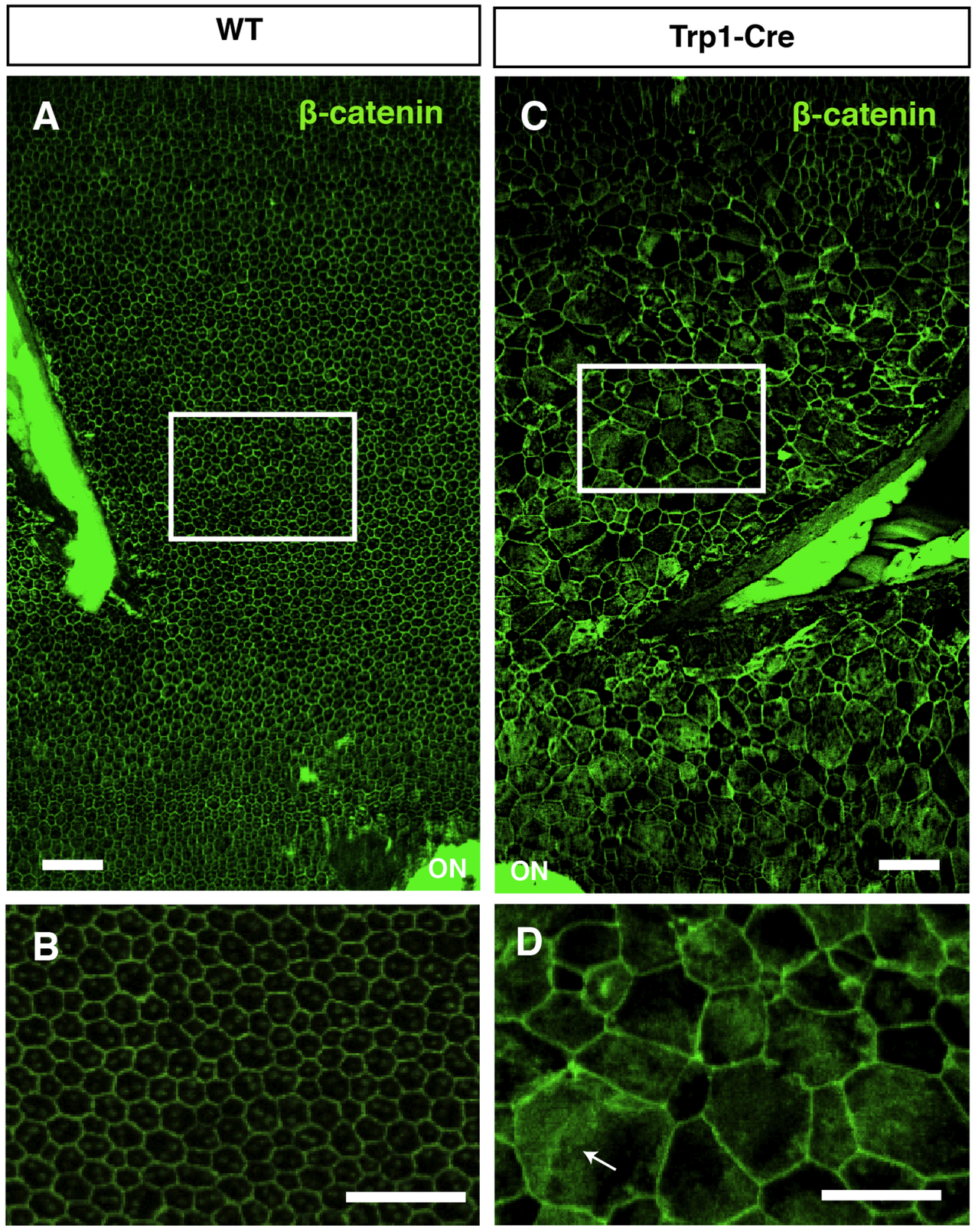
WT
Trp1-Cre
A
β-catenin
C
β-catenin
ON
ON
B
D

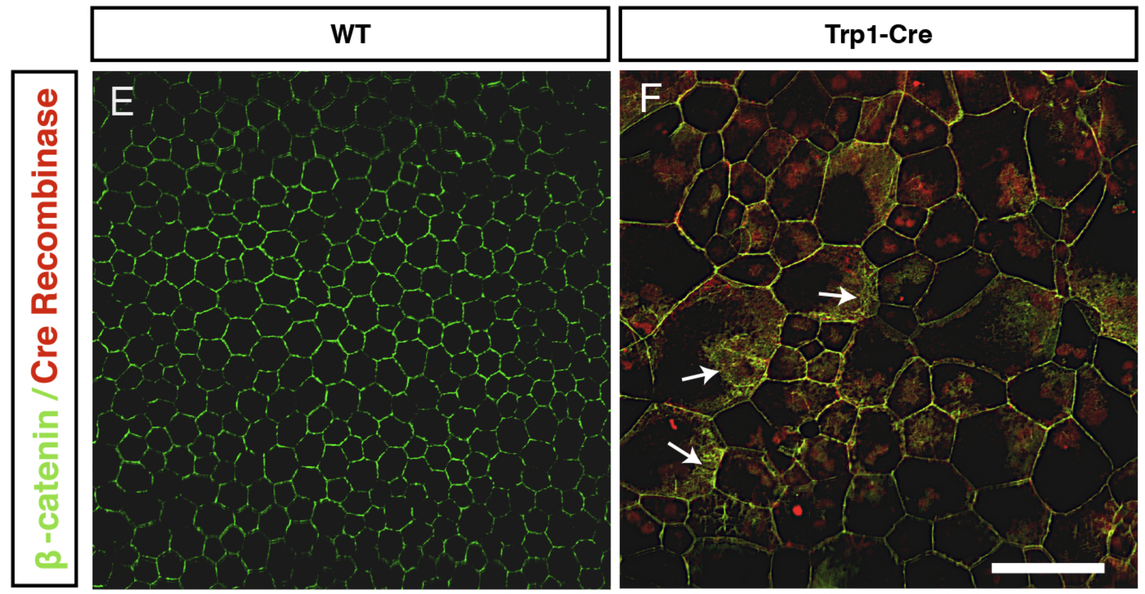
WT
Trp1-Cre
β-catenin / Cre Recombinase
E
F

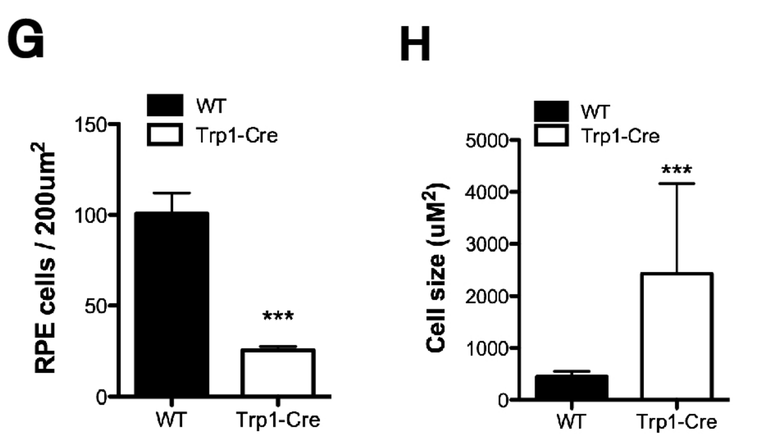
G
RPE cells / 200um2
150
100
50
0
WT
Trp1-Cre
***
H
Cell size (uM2)
5000
4000
3000
2000
1000
0
WT
Trp1-Cre
***
I
Cell Perimeter (uM)
400
300
200
100
0
WT
Trp1-Cre
***

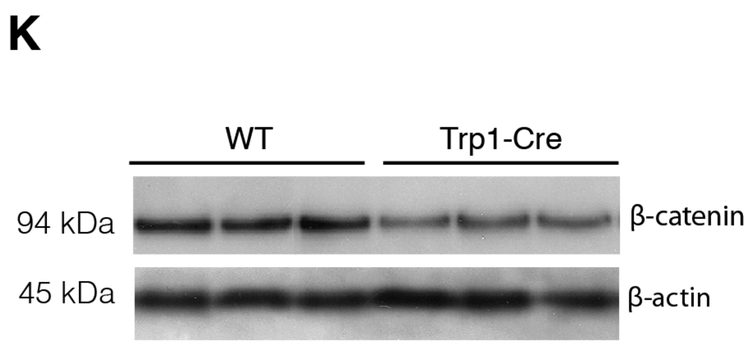
K
WT
Trp1-Cre
94 kDa
β-catenin
45 kDa
β-actin
L
β-catenin expression (A.U)
125
100
75
50
25
**
Wild Type
Trp1-Cre

Figure 3

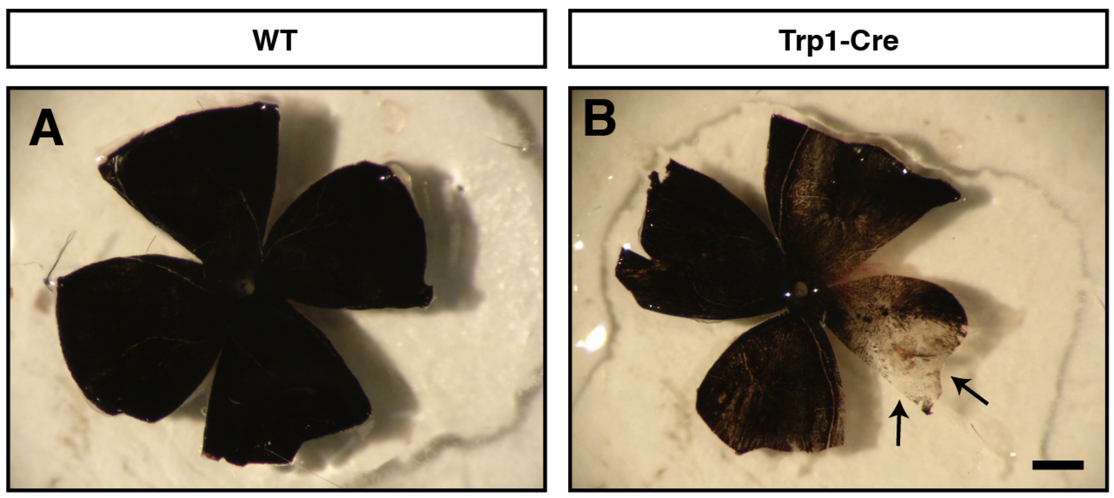
WT
Trp1-Cre
A
B

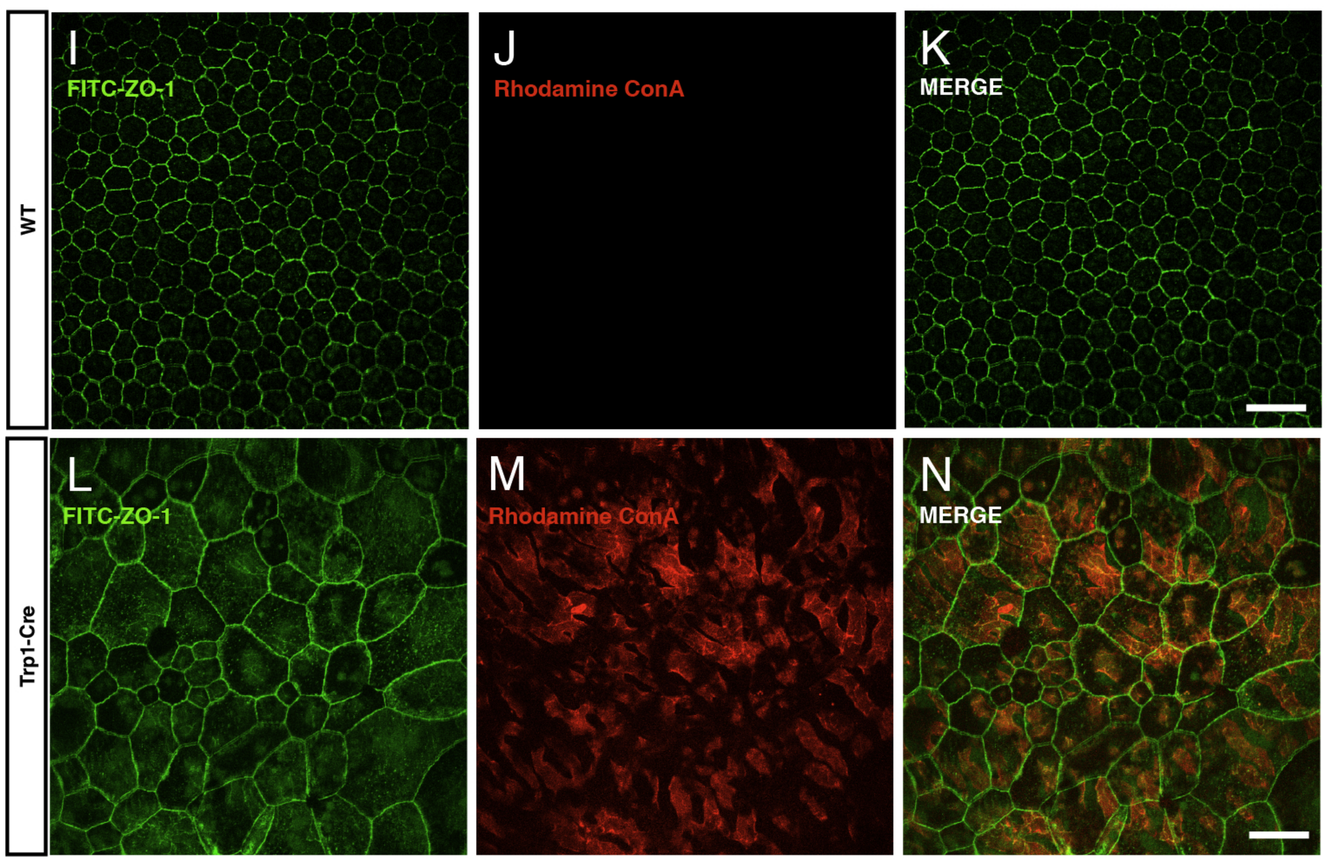
WT
I
FITC-ZO-1
J
Rhodamine ConA
K
MERGE
Trp1-Cre
L
FITC-ZO-1
M
Rhodamine ConA
N
MERGE

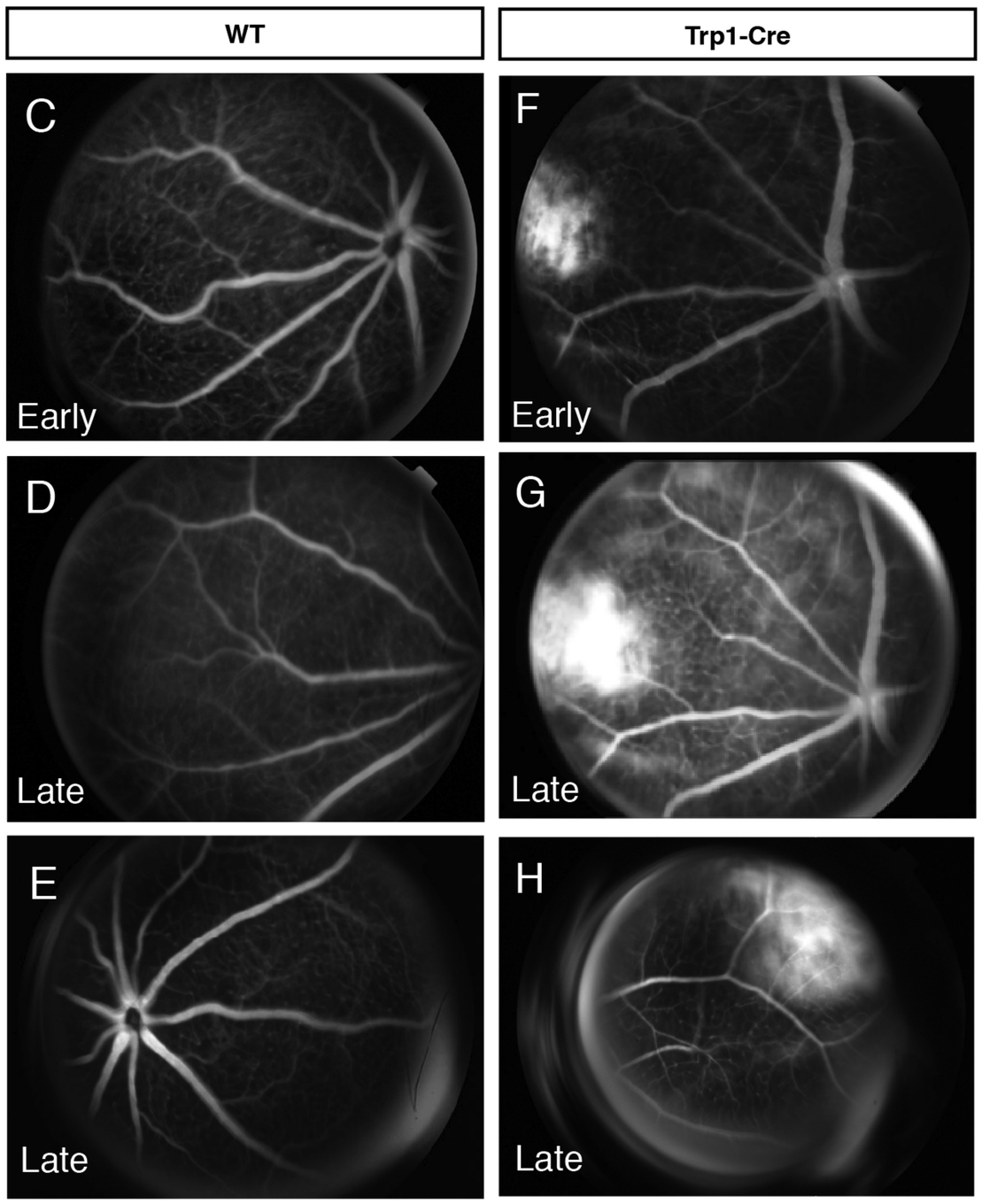
WT
Trp1-Cre
C
Early
F
Early
D
Late
G
Late
E
Late
H
Late

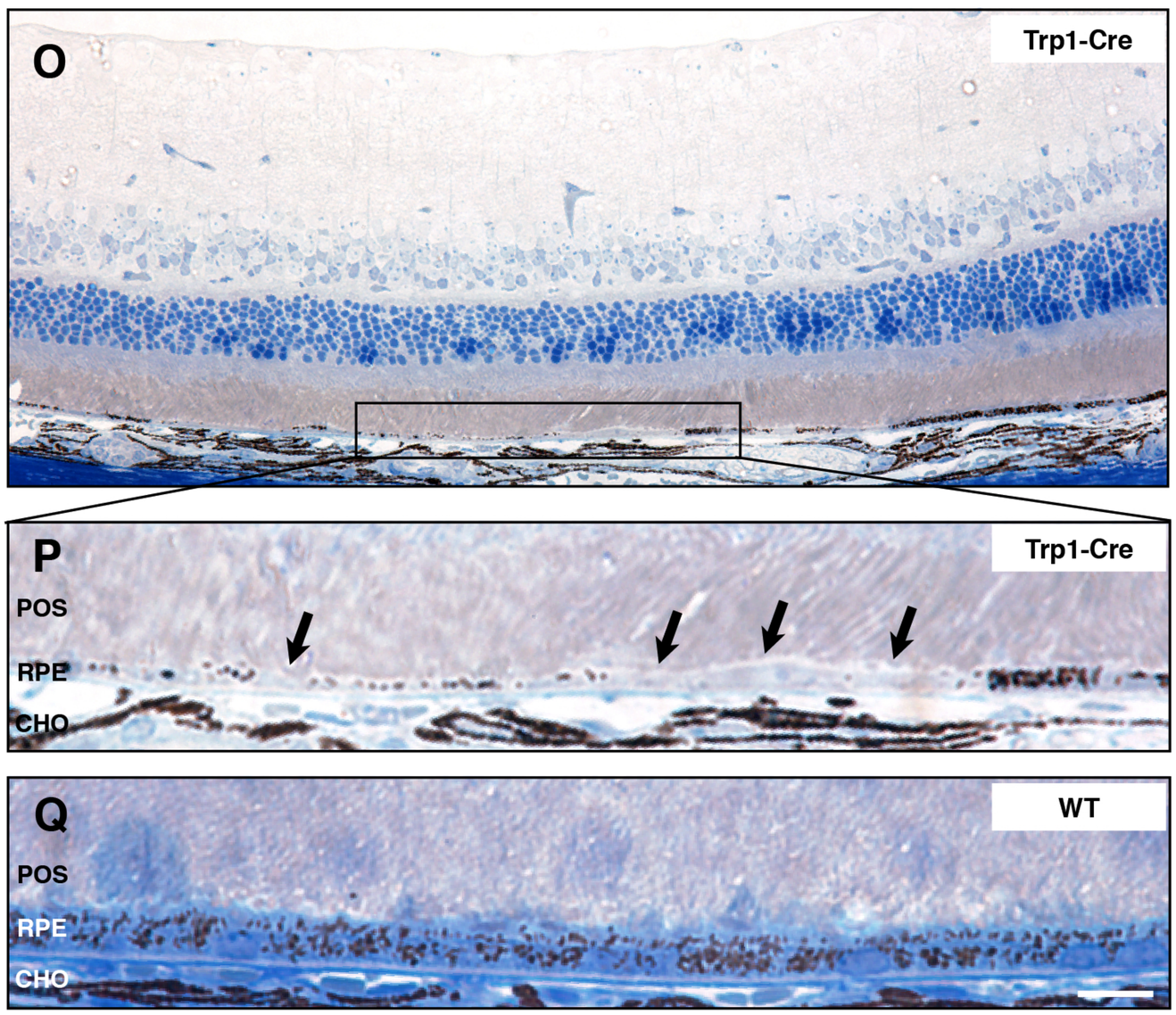
O
Trp1-Cre
P
Trp1-Cre
POS
RPE
CHO
Q
WT
POS
RPE
CHO

Figure 4

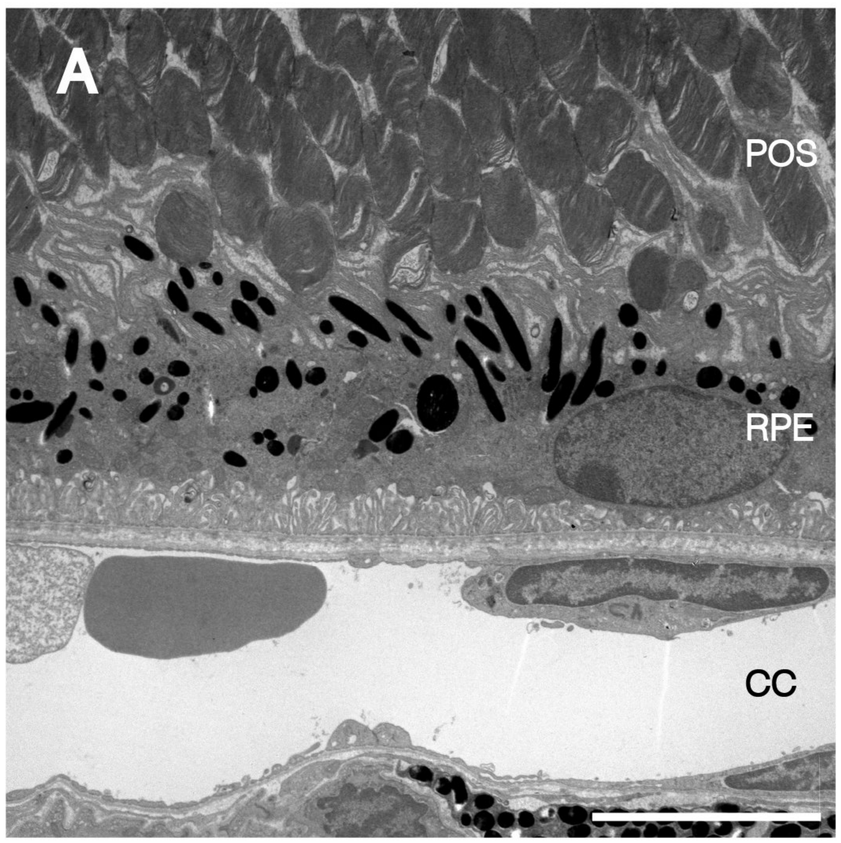
A
POS
RPE
CC

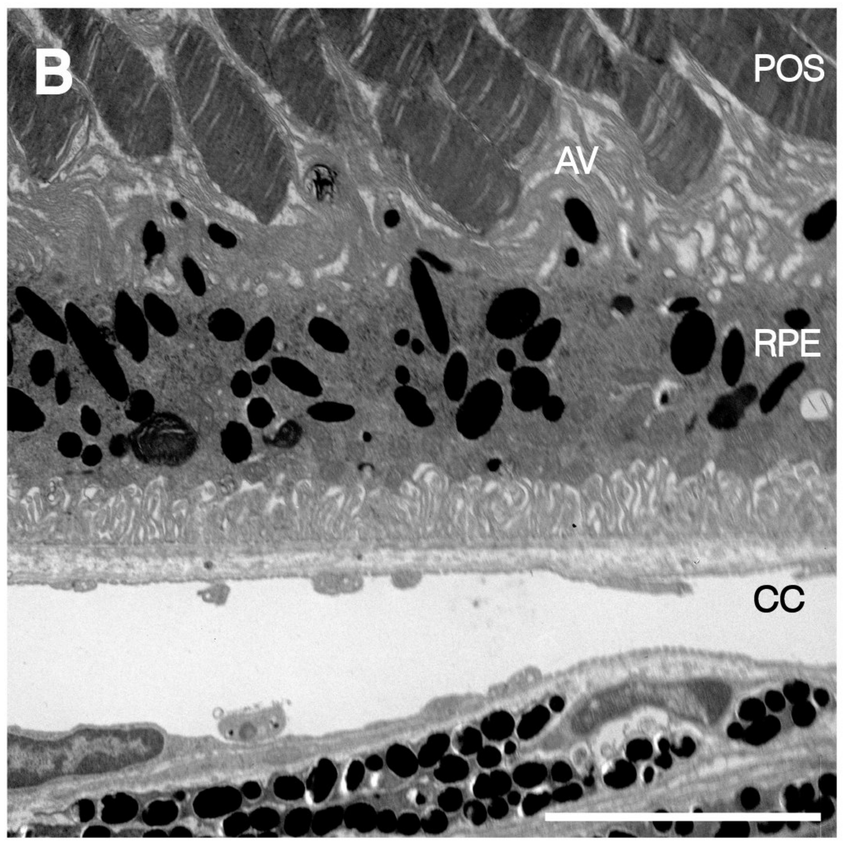
B
POS
AV
RPE
CC

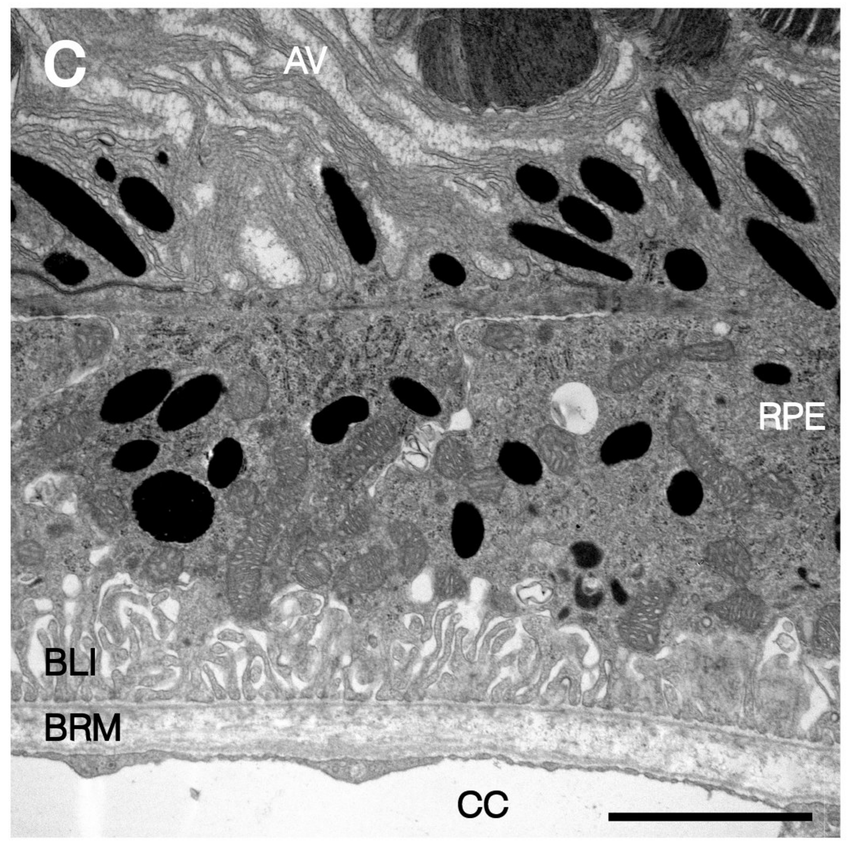
C
AV
RPE
BLI
BRM
CC

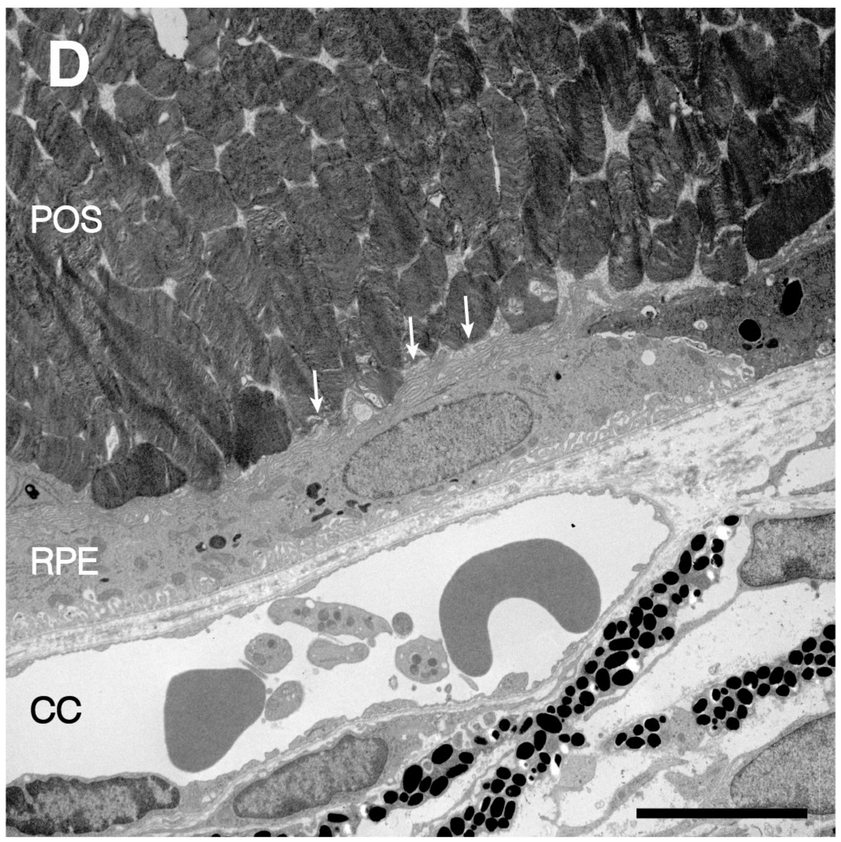
D
POS
RPE
CC

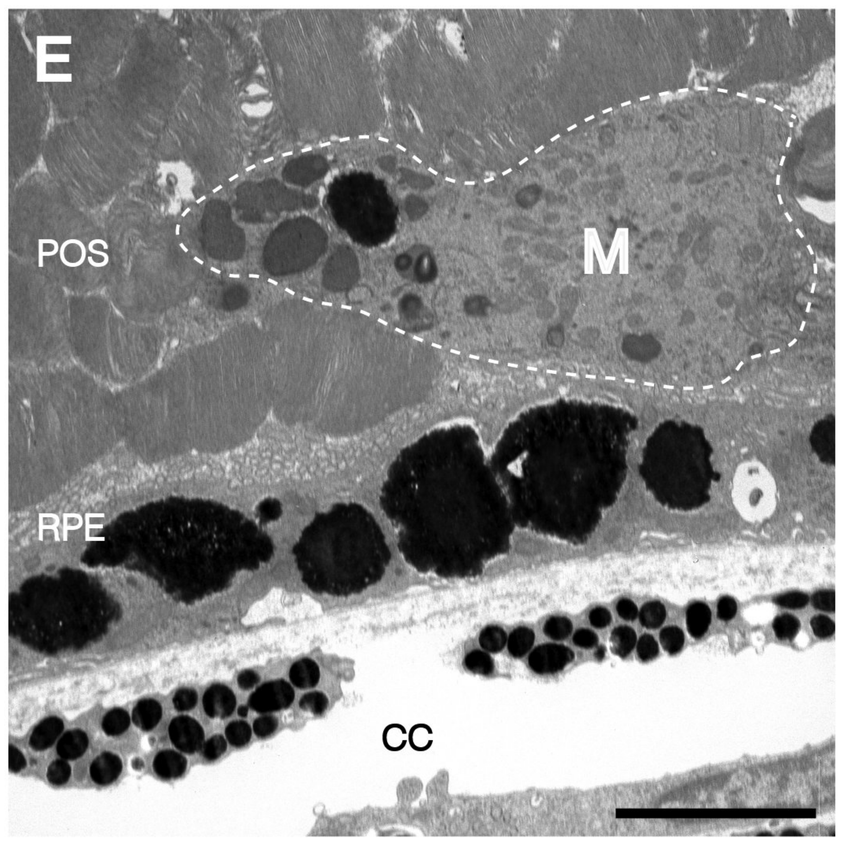
E
POS
M
RPE
CC

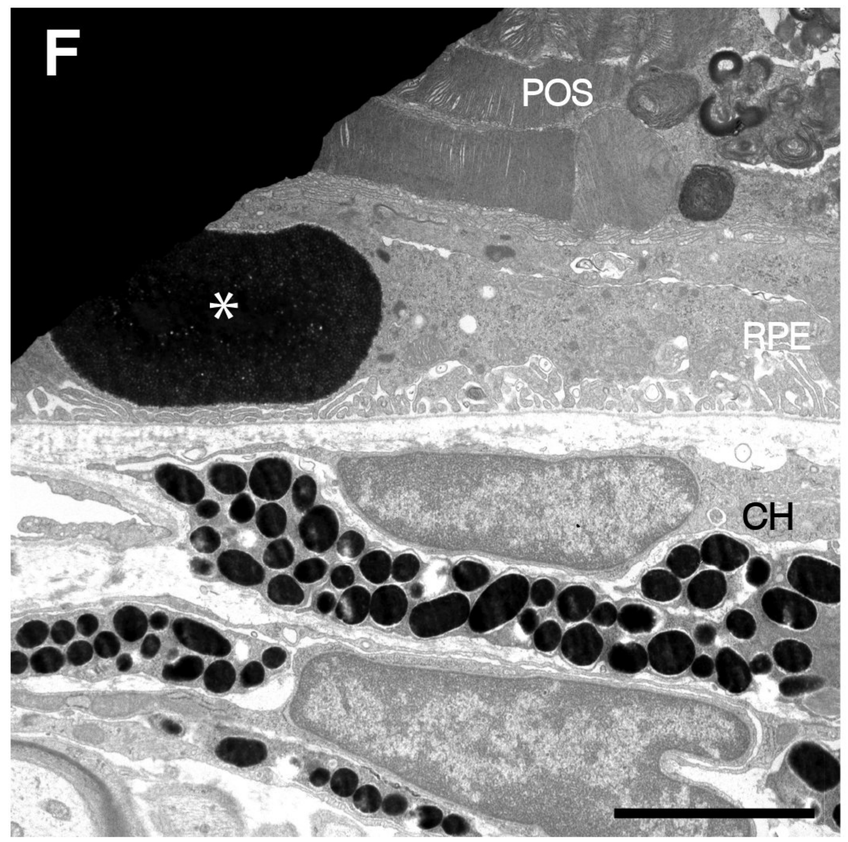
F
POS
*
RPE
CH

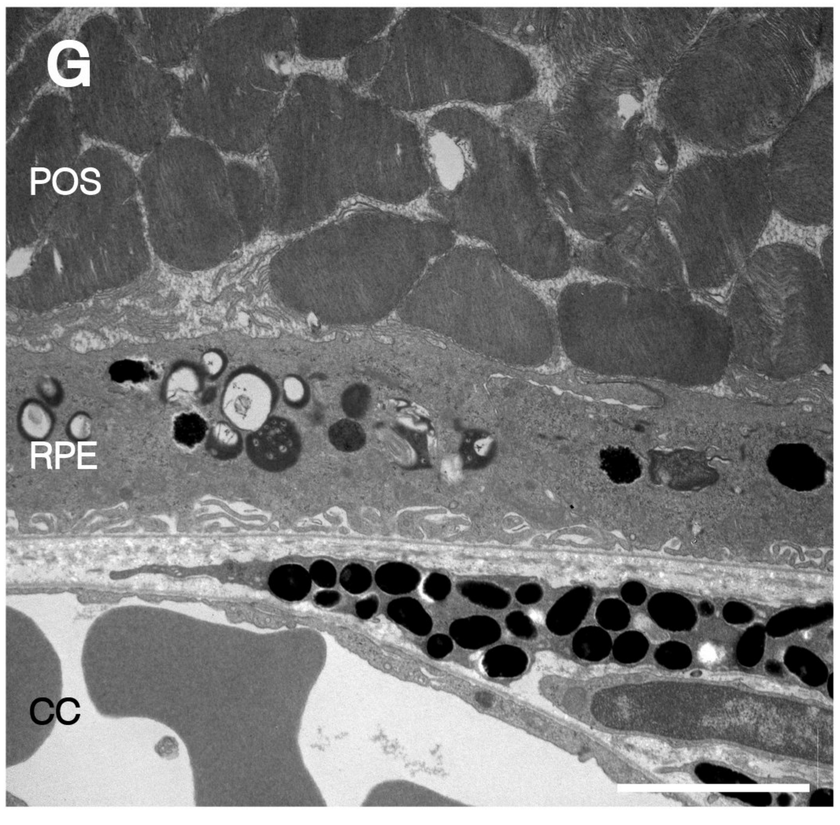
G
POS
RPE
CC

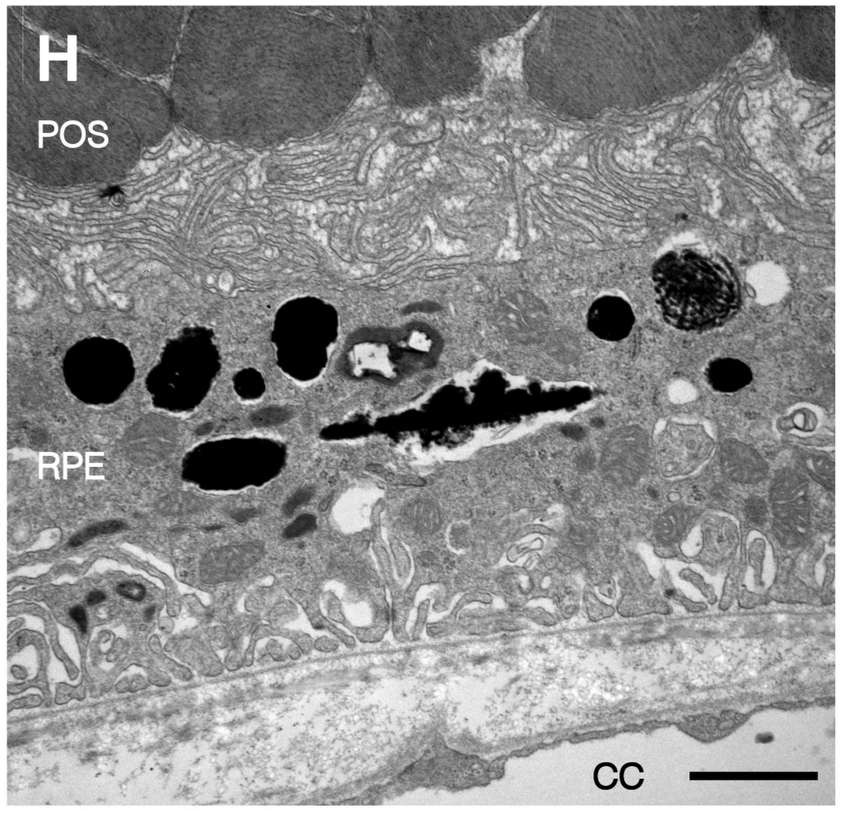
H
POS
RPE
CC

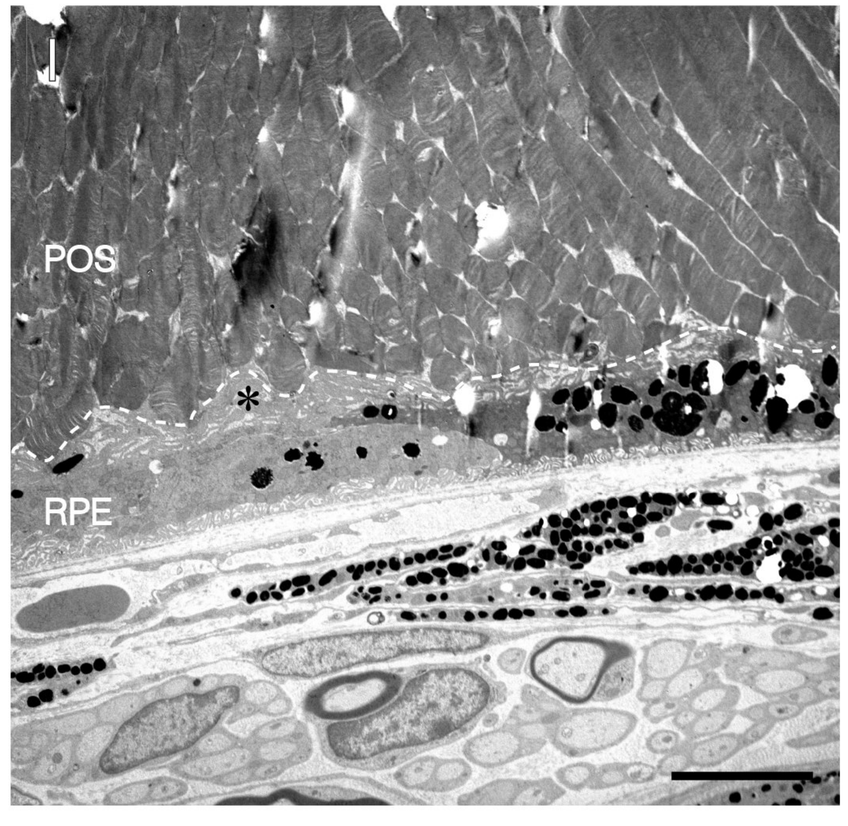
POS
*
RPE

Figure 5

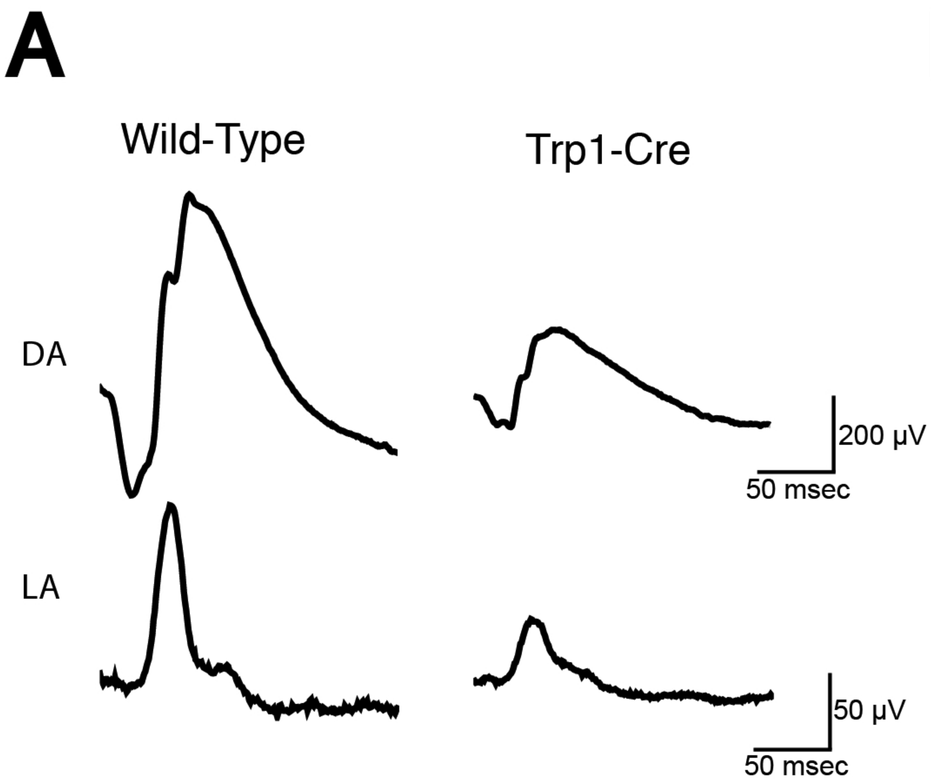
A
Wild-Type
Trp1-Cre
DA
LA
200 µV
50 msec
50 µV
50 msec

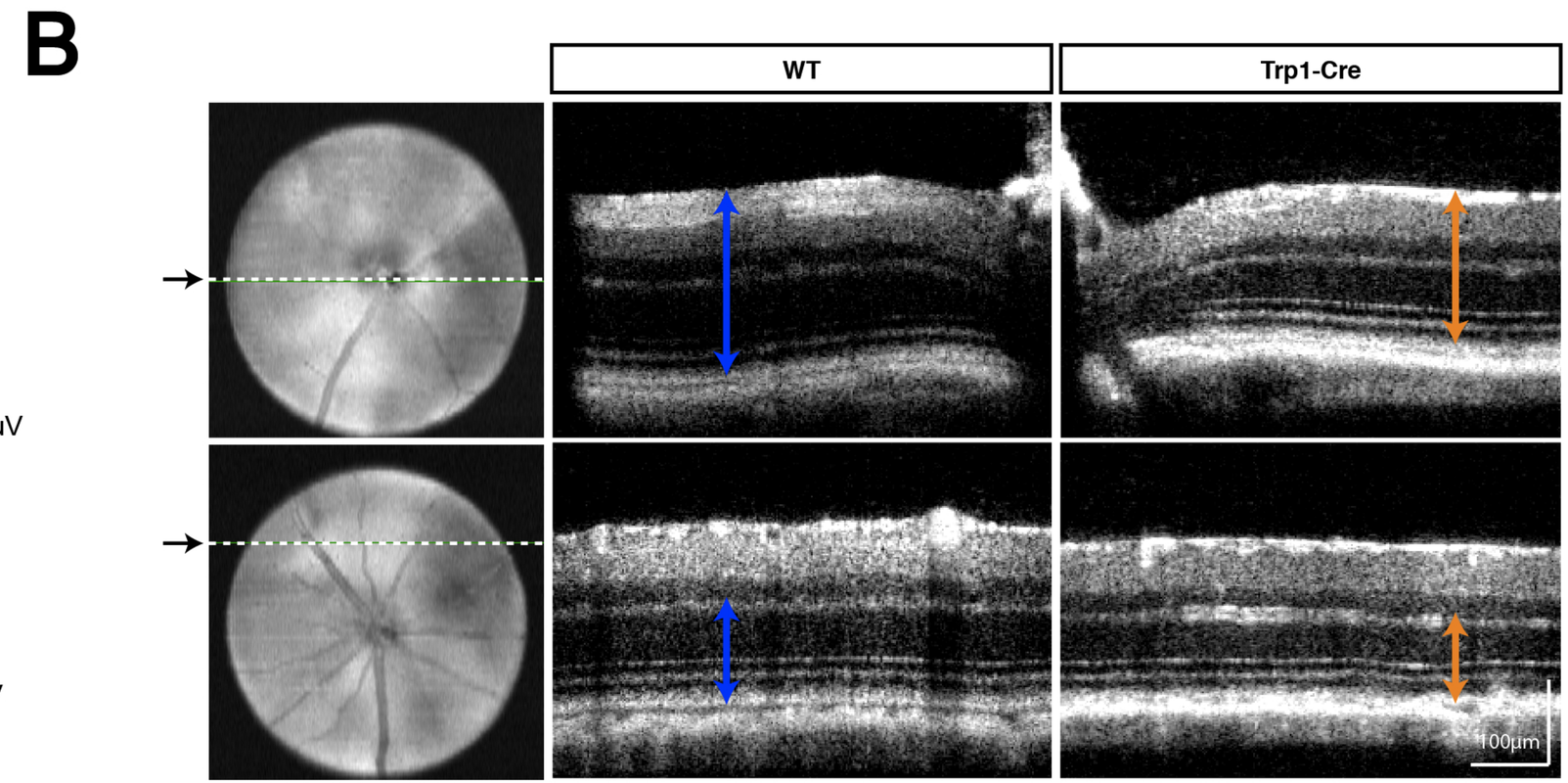
B
WT
Trp1-Cre
100µm

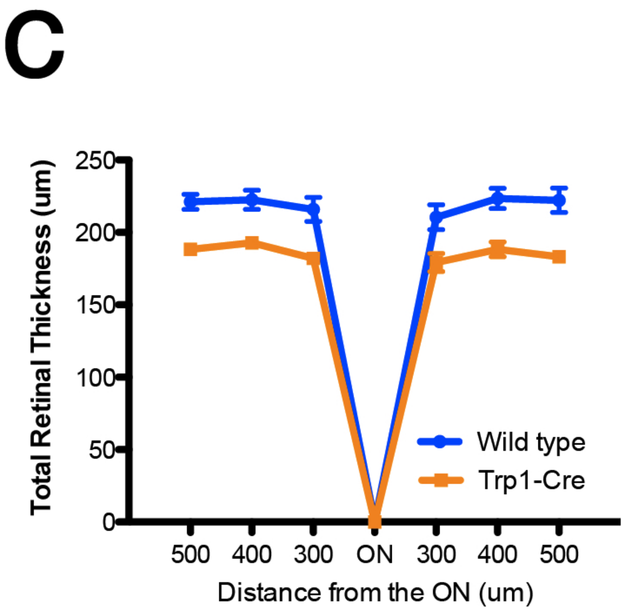
C
Total Retinal Thickness (um)
250
200
150
100
50
0
500 400 300 ON 300 400 500
Distance from the ON (um)
Wild type
Trp1-Cre

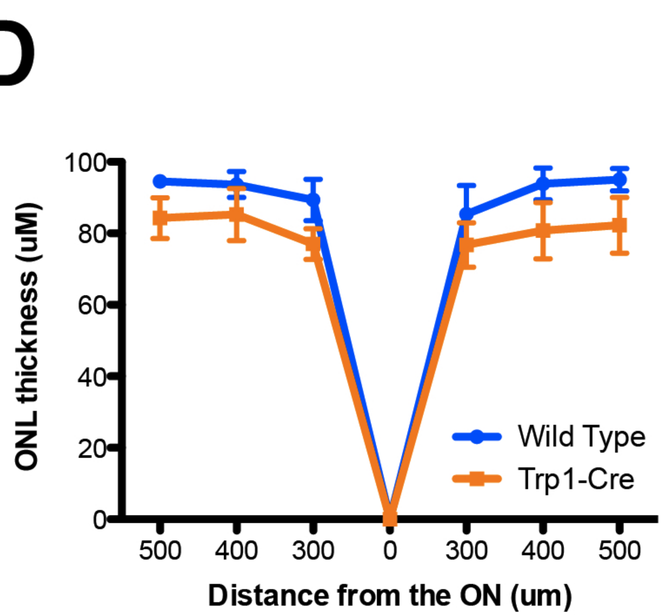
D
ONL thickness (uM)
100
80
60
40
20
0
500 400 300 0 300 400 500
Distance from the ON (um)
Wild Type
Trp1-Cre

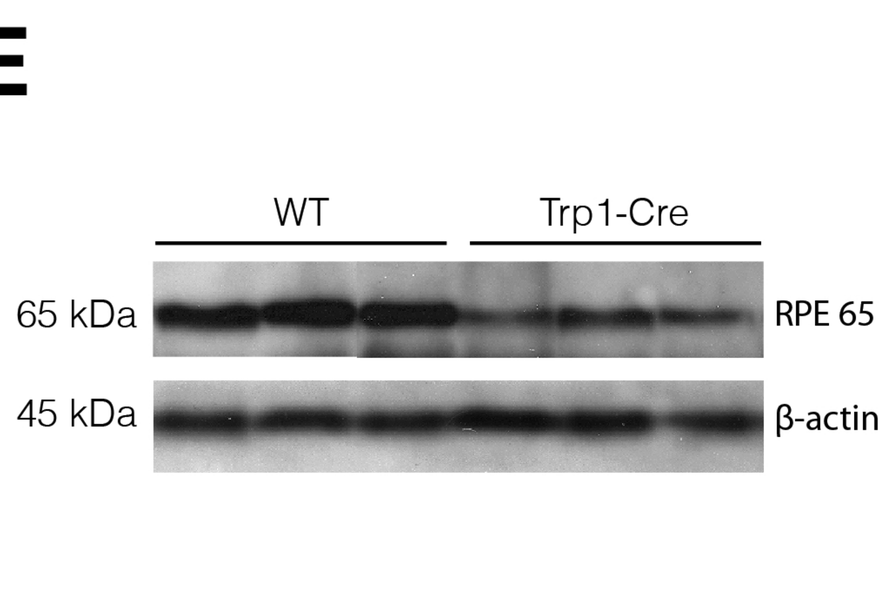
E
WT
Trp1-Cre
65 kDa
RPE 65
45 kDa
β-actin

Figure 6

Trp1-Cre

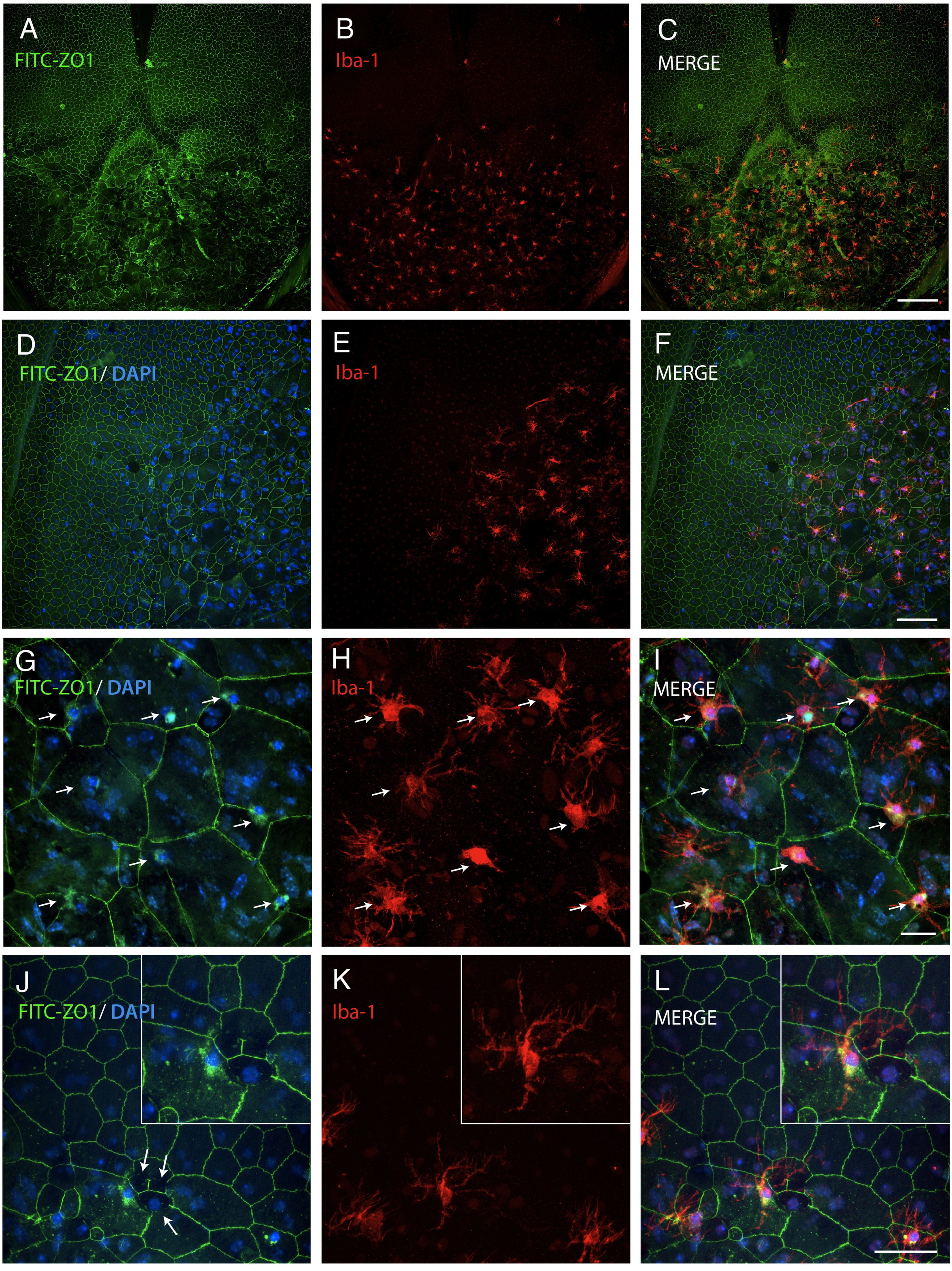

Supplemental Figure 1

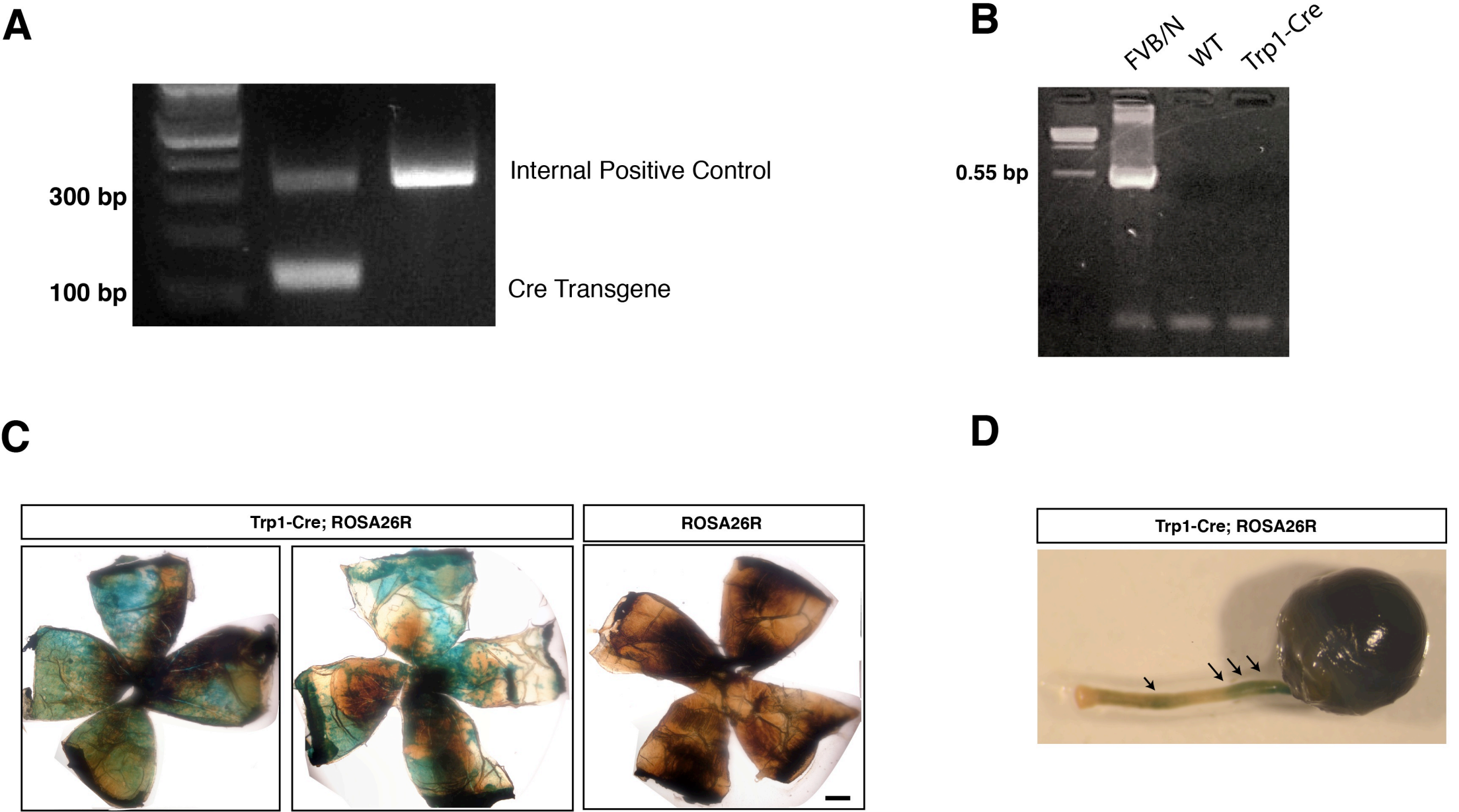

Supplemental Figure 2

A

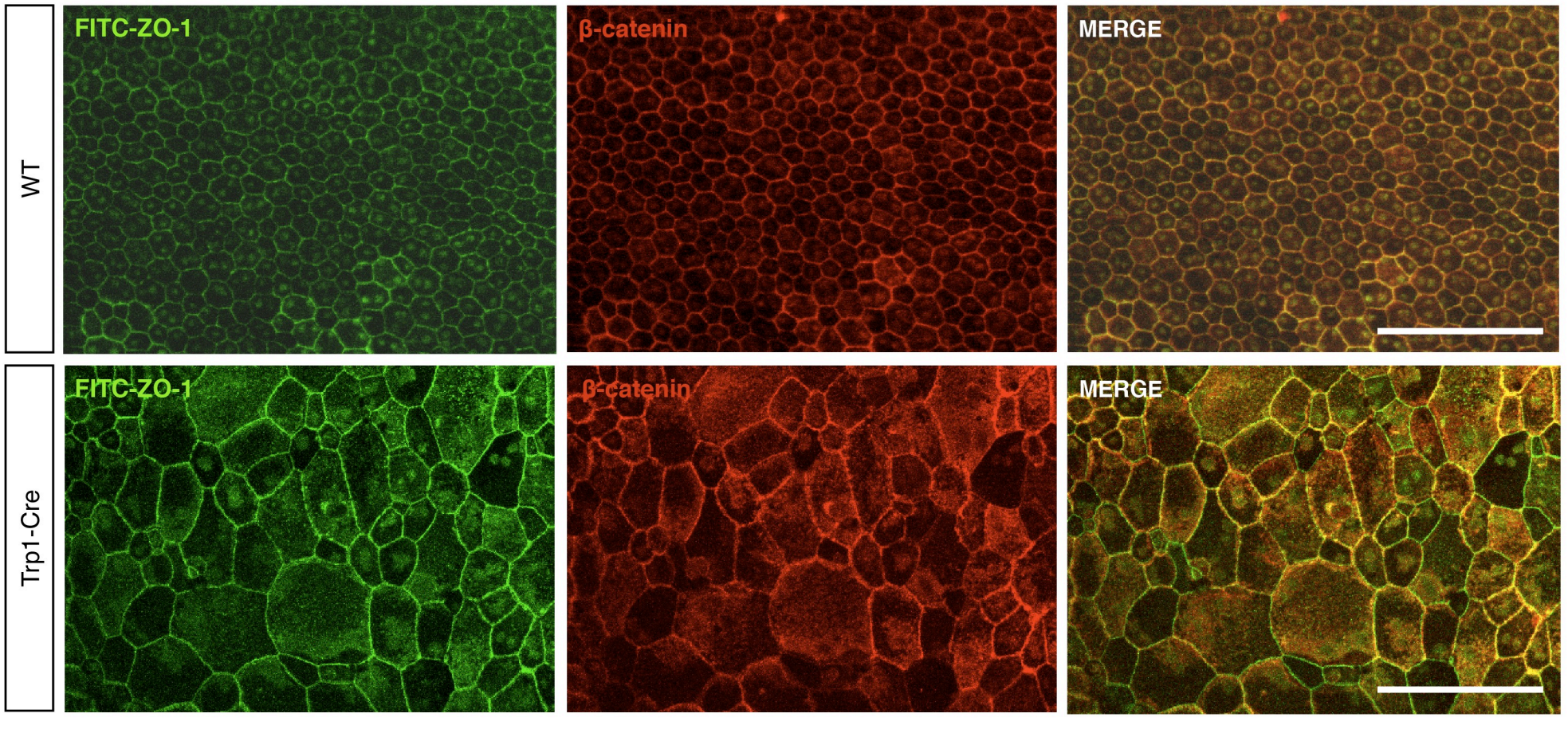

B

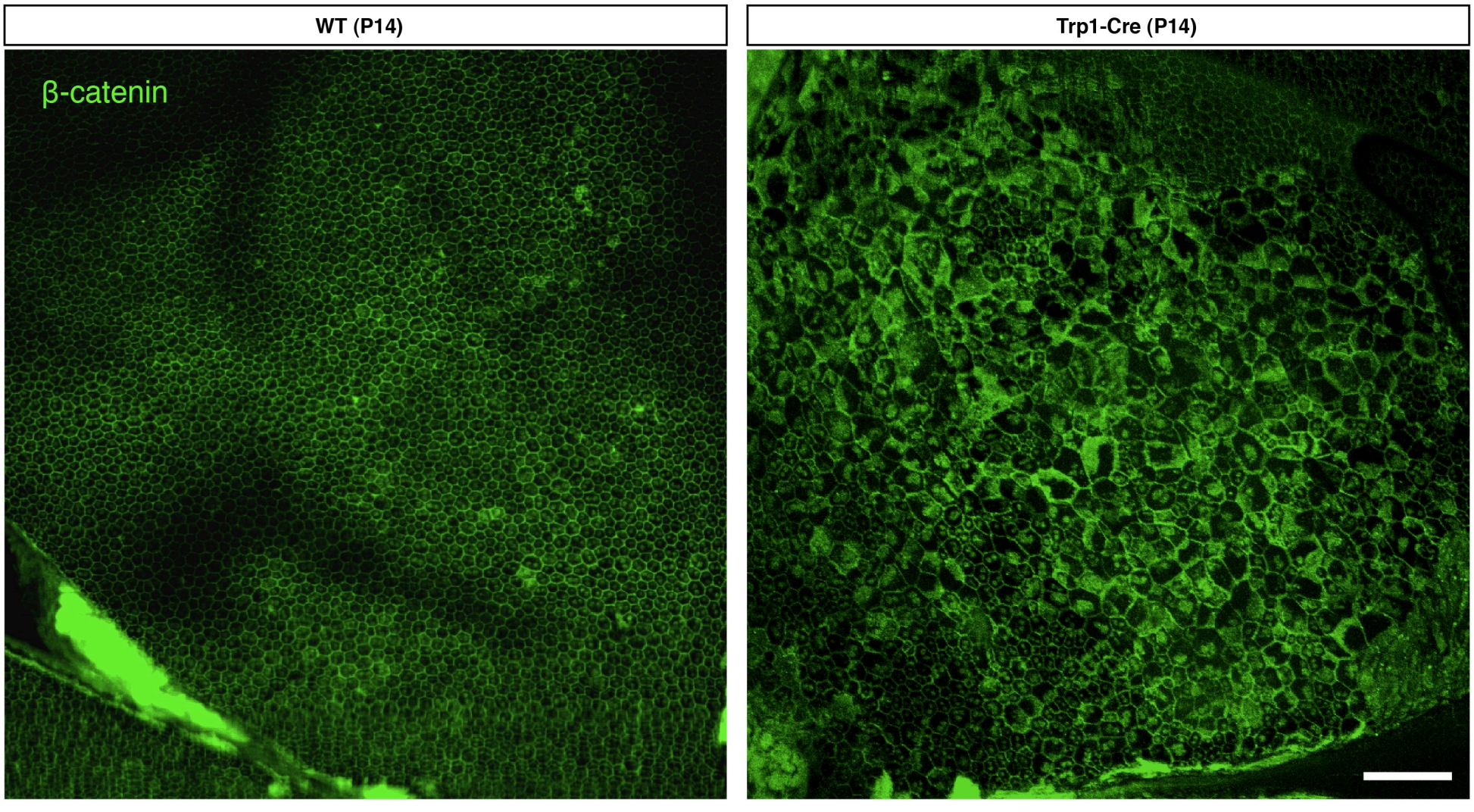

Supplemental Figure 3